August 1965

First Quarterly Report | *Covering the Period 14 May 1965 to 14 August 1965*

RESEARCH ON COLD CATHODES

Prepared for:

NATIONAL AERONAUTICS AND SPACE ADMINISTRATION
GODDARD SPACE FLIGHT CENTER
GREENBELT, MARYLAND

CONTRACT NAS 5-9581

By: D. V. GEPPERT

SRI Project 5511

Approved: PHILIP J. RICE, MANAGER
PHYSICAL ELECTRONICS LABORATORY

J. D. NOE, EXECUTIVE DIRECTOR
ENGINEERING SCIENCES AND INDUSTRIAL DEVELOPMENT

Copy No. 12

ABSTRACT

15600

In the first section of the report the requirements for the surface film, for the semiconductor, and for the vacuum are presented in detail. The major requirements are:

A. Metal Surface Film

1. It must be possible to activate the film with a low-work-function coating so that the vacuum barrier is low ($\lesssim$ 1.3 ev).
2. The surface film must make a blocking contact with a high barrier ($\gtrsim$ 1.3 ev) with the semiconductor used.
3. The hot-electron mfp (mean-free-path) should be as long as possible.
4. It must be possible to deposit a continuous film on the order of 100Å in thickness.
5. The sheet resistance of the film should be as low as possible.

B. Semiconductor

1. A large band-gap ($\gtrsim$ 2 ev) is required to minimize hole injection from the metal surface film.
2. It must be possible to make an ohmic contact, which means it is necessary to dope the crystal n-type to a reasonably low resistivity.
3. The semiconductor must be available in reasonably large single crystals.

C. Vacuum

1. An oil-free vacuum system is required to produce a clean metal/semiconductor junction and a clean vacuum surface for the cathode.

2. A vacuum of $\sim 10^{-9}$ to 10^{-10} torr is believed necessary during and at all times subsequent to fabrication of the cathode structure. This is necessary to achieve and to maintain a low vacuum work function.

Gallium phosphide crystals have been intensively studied for application to the surface-barrier cold cathode. Hall measurements and optical transmission measurements have been made and the results analyzed for two large high-quality crystals obtained from two different sources.

Lapping, polishing, and etching studies have been conducted on these crystals to determine optimum surface preparation procedures. It has been found that ohmic contacts to GaP can be produced by alloying lead (Pb) or Te-doped Ag to the crystal surface. It has also been found that evaporated Pt forms a blocking contact with a high barrier ($\sim$ 1.45 ev) to GaP. These diodes were not prepared in an oil-free vacuum system, and electrical measurements emphasize the need for an oil-free system. Such a system has been completed and is now ready for operational use.

Two Pt/evaporated BaO phototubes made recently indicate that such a combination produces a work function larger than 1.5 ev. Thus the simple system GaP-Pt-BaO does not appear feasible. The systems GaP-Pt-Ag-BaO or GaP-Pt-Ta-BaO look promising, however. The system GaP-W-BaO is currently undergoing evaluation.

Long life has been demonstrated for GaP-Pt diodes and for Ag-BaO phototubes. The GaP-Pt diodes are undergoing dynamic operational life tests and have not changed significantly after 1000 hours. The Ag-BaO photosurface is unchanged after nine months.

Author

CONTENTS

ILLUSTRATIONS

TABLES

I INTRODUCTION

The objective of this program is to perform research on semiconductor/metal, hot-electron cold cathodes. The hot electrons are generated in a thin metal surface film by forward-biasing a rectifying semiconductor/metal diode. The metal film is on the order of 50-to-100 Å in thickness and is activated by a low-work-function coating to reduce the vacuum barrier below the semiconductor/metal barrier. Energy diagrams for the cathode, with and without bias, are shown in Figs. 1(a) and 1(b). The dimensions of the structure are not drawn to scale. The thickness of the metal film is exaggerated for reasons of clarity. Referring to Fig. 1(b), a portion of the hot electrons emitted over the top of the barrier into the metal film traverse the film ballistically and enter the vacuum. Most of those electrons that become scattered in the metal film are lost, however; and these electrons create a bias current for the device.

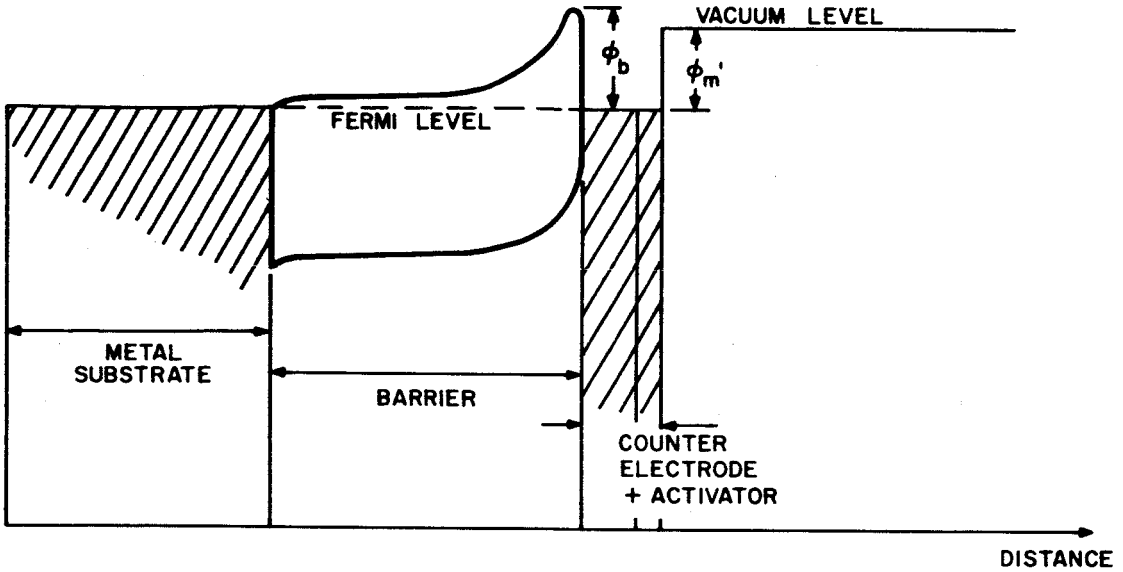

(a) ENERGY VS. DISTANCE OF SURFACE BARRIER CATHODE WITHOUT BIAS.

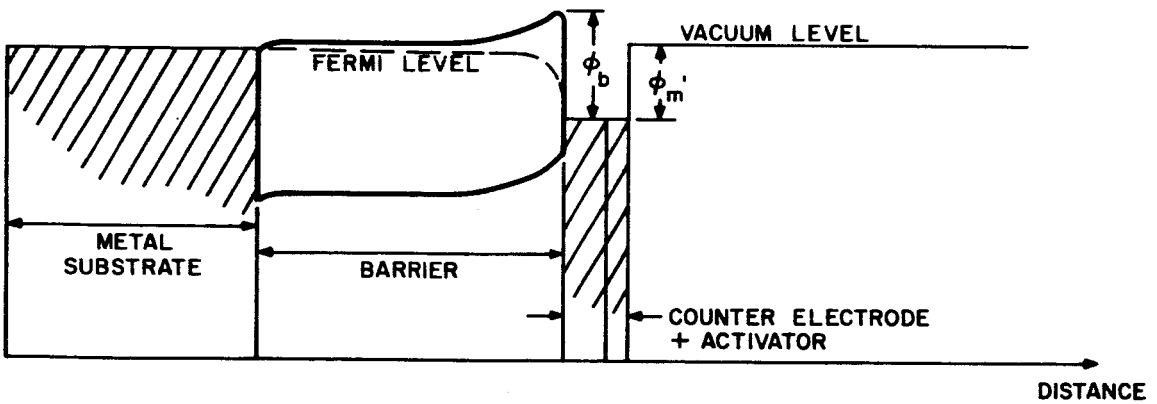

(b) ENERGY VS. DISTANCE OF SURFACE BARRIER CATHODE WITH BIAS.

FIG. 1 ENERGY DIAGRAM OF SURFACE BARRIER CATHODE

II DISCUSSION

A. DISCUSSION OF REQUIREMENTS

Referring to Fig. 1(a), it is evident that a primary requirement in the metal/semiconductor cathode structure is that φ_b be greater than φ_m', where φ_m' denotes the work function of the metal-vacuum interface. Owing to the surface treatment, the value of φ_m' will, in general, be less than the bulk metal work function φ_m. Electrons which are emitted over the surface barrier into the metal then have sufficient energy to overcome the potential step at the metal surface and can emerge into the vacuum.

All reported experimental and theoretical evidence points to the fact that the lowest obtainable work functions for metal films are greater than 1 ev.[1-6]* Evaporated monolayers of cesium on metal films produce low-work function surfaces with φ_m' on the order of 1.6 ev.[1-4] Experiments with evaporated layers of BaO on refractory metals indicate that work functions as low as 1.3 ev can be obtained.[5,6] Various complex substances with work functions of about 1.0 ev have been prepared[7] but these are generally unsuitable for the present purpose, since they are usually semiconductors rather than metals, and are conveniently prepared only in relatively thick films, on the order of 1000 Å.[8,9] This conflicts with the requirement, to be discussed below, that the metal film be very thin ($\sim$ 100Å).

1. Metal Film

The metal film must satisfy three primary requirements. In addition to the requirement that the metal be capable of producing a low-work function φ_m' upon suitable treatment of its surface, it must have a hot electron attenuation length, L_e, which is great enough to

---

*References are listed at the end of the report.

allow most of the electrons emitted over the surface barrier to reach the metal-vacuum interface. The third requirement is that the metal must produce a high surface barrier at the metal-semiconductor interface. This requirement will be discussed more fully in the following section.

Measurements performed in this laboratory indicate that thin evaporated films of BaO on refractory and noble metal surfaces are capable of producing the low values of φ_m' which are necessary for the fabrication of a successful cathode. This approach is based largely upon the results obtained by Moore and Allison,[5] who measured the thermionic work functions of W, Mo, Ta and Zr coated with BaO films of various thicknesses. The results on W, Mo, and Ta indicate thermionic work functions as low as 1.0 ev, for the thickest BaO films ($\sim$ 20 monolayers). This limiting work function is presumably that of bulk BaO. Thin films ($<$ 1 monolayer) of BaO on W produce work functions of about 1.3 ev. The most promising results obtained to date in this laboratory have been obtained with BaO-activated Ag films. Values for φ_m' of about 1.35 ev have been measured for this case.

The attenuation length L_e of electrons in a few metals has been studied experimentally and theoretically by a number of workers. Some of the references to the experimental work are cited.[10-15] Gold has been investigated in greatest detail, and the latest measurements[15] indicate that $L_e = 350\text{Å}$ for electrons 0.95 ev above the Fermi level. This number probably represents an upper limit for the value of L_e for most metals at this energy. Since the probability is $\exp(-x/L_e)$, that an electron will travel a distance x in the metal film without scattering, it can be appreciated that the thickness of the metal film in the proposed cathode must be less than L_e so that most of the electrons emitted over the surface barrier can reach the vacuum interface. This means that extremely thin ($\sim 100\text{Å}$) films are required, and that metals which are to be considered for use in the cathode must be easily deposited in thin, continuous films. The refractory metals seem to meet this requirement most satisfactorily, since they show the least tendency to agglomerate in thin films. Fortunately, the refractory metals have relatively

large bulk work functions which are required to produce high surface barriers at the metal-semiconductor interface.

Materials which can withstand the temperatures encountered in tube bake-out are desirable from the standpoint of the fabrication of an electron tube containing a metal-semiconductor surface barrier cathode. Again, refractory metals are the most promising in this respect, since they show less tendency to diffuse into the semiconductor at elevated temperatures than do non-refractory metals.

Another requirement on the metal, of lesser importance than those just discussed, is that it have a low sheet resistance in thin films. This requirement is based on the necessity for preventing large transverse voltage drops in the film when it is biased for normal operation of the cathode, and is analogous to the requirement that the lateral voltage drop in the base of a junction transistor be minimized. The sheet resistance of metallic films is strongly dependent on the substrate material, the manner in which the film is deposited, and any treatment of the film subsequent to deposition, e.g., annealing. Observations of film sheet resistivity in this laboratory have been made on Pt films; and for 100Å films deposited on a room temperature glass substrate; resistivities of the order of 100Ω/□ are indicated. This figure is probably representative of the resistivities to be expected for refractory metal films of the same thickness. If this resistivity proves to be too high, it might be necessary to evaporate a grid pattern of thicker material on the metal film in order to provide low-resistance current paths to the entire film.

2. Semiconductor Requirements

In view of the requirement that $\varphi_b > \varphi_m'$, an important property of any semiconductor considered for use in the proposed cathode is its ability to form high surface barriers with metals. Since the height φ_b of the surface barrier in an n-type semiconductor/metal contact cannot exceed the band gap E_g, a general requirement is that E_g be greater than the barrier height desired. Mead and Spitzer[16] have shown for a large number of semiconductors that the general relation $\varphi_b \approx \frac{2}{3} E_g$ is valid

for the n-type semiconductor-metal contact. The assumption is made here that the Fermi level at the interface is pinned by surface states at $\frac{1}{3} E_g$ above the valence band edge, regardless of which metal is used. A more detailed analysis of the dependence of φ_b on surface states and the metal work function has been made by Cowley and Sze,[17] but the result of Mead and Spitzer provides a convenient "rule of thumb" for use in the preliminary evaluation of a particular semiconductor. According to this rule, the band gap of the semiconductor must be greater than 1.5 times the desired surface barrier height. Since we have indicated that the lowest obtainable metal-vacuum work functions, φ_m', are in the range 1.0 to 1.3 ev, this places a lower limit of about 1.3 ev on φ_b and $1.5 \times 1.3 \approx 2$ ev on E_g, in order that the condition $\varphi_b > \varphi_m'$ be satisfied. This restriction eliminates many of the semiconductors of greatest current technological importance, e.g., Si, Ge, GaAs.

Some semiconductors which do meet this restriction[18] are gallium phosphide, cadmium sulfide, and zinc oxide. Gallium phosphide is currently under investigation in this laboratory, and the results for this material show that it is capable of producing barriers higher than 1.3 ev with high work-function metals (e.g., Pt); these results are in agreement with work previously reported by other workers.[17,19] Zinc oxide has also been the subject of investigation,[20] but the results with this material were less promising. Because the devices investigated were prepared in an oil-diffusion vacuum station, however, the barrier heights inferred from measurements of the electrical behavior of the diodes may not have been correct. It may therefore be worthwhile to reopen the investigation of ZnO, using diodes prepared in the Vac-Ion vacuum system which has recently become available.

Blocking contacts on cadmium sulfide have been investigated in great detail by Goodman,[21] and by Spitzer and Mead.[22] With the exception of Pt on chemically cleaned crystals, barriers fabricated on CdS were all smaller than 1 ev. Platinum on chemically cleaned crystals produced a barrier height of 1.20 ± 0.15 ev. Therefore, with the possible exception of the platinum diode, CdS is not a candidate for the semiconductor in

this program. A great number of semiconductors with band gaps greater than 2.0 ev are known;[18,23] but for a variety of reasons, some of which will be discussed below, most of them are unsuitable for investigation in the present program.

In order for a wide-band-gap semiconductor to be useful in this program, it must be capable of being doped n-type, with a reasonably low resistivity. This requirement arises from the necessity for establishing ohmic contacts to the material (essentially a doping process), and from the requirement for a barrier to electrons flowing into the metal [Fig. 1(a)]. This constraint eliminates a great number of semiconductors and all insulators.

Semiconductors to be used in the current program must of course be available in single crystals which are large enough to provide surfaces upon which to form ohmic and blocking contacts. This requirement has proven to be an obstacle to the investigation of SiC as produced in the SRI Materials Research Laboratory. This program is expected to produce larger single crystals of β-SiC in the near future, however; and as these become available, the investigation of surface barriers will be continued. In view of the extensive effort being devoted in various industrial research laboratories to the growth and investigation of single crystal wide-band-gap semiconductors, it is also anticipated that many more of these materials will become available in the near future. This is an encouraging prospect, in view of the necessarily restrictive requirements placed on semiconductors suitable for use in the present cathode program.

3. Vacuum Requirements

The need for a high, clean vacuum has been well established in the production of low-work-function surfaces and coatings. Particularly notable in this respect are photoemissive surfaces for phototubes and investigative programs. Before the advent of modern, oil-free vacuum technology, such vacuums could only be produced by an elaborate and complicated schedule of bake-out and degassing, after which the apparatus which required a high vacuum was sealed permanently in a glass

envelope. A further increase in vacuum can often be obtained by flashing a getter in the tube. The use of such experimental techniques in investigations of surface phenomena which depend on a large number of parameters has obvious disadvantages, primarily the relatively long time required to produce a single device upon which one can perform measurements. The Vac-Ion vacuum system recently acquired by this laboratory is expected to eliminate many of the complicated fabrication procedures involved in the experiments on low-work function coatings with BaO. It has been necessary in the work described in past reports[20] to conduct BaO experiments in sealed, gettered glass envelopes, produced by the methods described above. It is now anticipated that such experiments can be set up in a matter of hours using the Vac-Ion system. The ultimate vacuum of the Vac-Ion system is also much lower than that of an oil-diffusion pumped system, and vacuums of 10^{-10} torr should be obtained.

The importance of high vacuum has been more recently demonstrated in the investigation of the properties of metal-semiconductor surface-barrier diodes.[19] In general it is found that the methods for measuring barrier height φ_b give ambiguous results when applied to devices prepared in oil-diffusion pumped systems. This is recognized as being due to the formation of an interfacial film on the semiconductor substrate prior to the evaporation of the metal contact; films with thickness on the order of tens of Angstroms are sufficient to cause drastic changes in the capacitance behavior of the diodes.[19] Depending upon the sticking coefficient of the residual gas molecules, a monolayer of absorbed molecules can form in less than one second to a few seconds in a vacuum of 10^{-6} to 10^{-7} torr.[24] This observation emphasizes the need for much higher vacuums, on the order of 10^{-9} to 10^{-10} torr.

B. SEMICONDUCTOR STUDIES

1. Gallium Phosphide Crystals

Until quite recently, sizable, good-quality single crystals of gallium phosphide have not been available from any source. Two different gallium phosphide crystals have been obtained for evaluation, however. One crystal, obtained from Stanford University, is referred to as

Crystal No. 1. A second crystal, obtained from the Monsanto Chemical Co., is referred to as Crystal No. 2. The Monsanto Chemical Co. is the only commercial source of sizable single crystals of gallium phosphide known at present.

a. Crystal No. 1

Crystal No. 1 is approximately 15 mm square and 0.5 mm thick and was produced by a process developed at Stanford University. This crystal was made in an open-tube flow system using purified hydrogen carrier gas to pick up phosphorus trichloride vapor from a bubbler saturator. The phosphorus trichloride and hydrogen then enter the reaction tube and react with liquid gallium metal, which is held in a quartz boat at 930°C, to form the reactants. These flow down the tube and combine on a gallium arsenide substrate to form gallium phosphide at a temperature of 810°C in a zone with a temperature gradient of about 20°C per cm. Crystals may also be conveniently doped by adding suitable doping elements to the hydrogen gas stream during growth.

During the deposition, the gallium arsenide substrate is etched by the reactant gases; and for depositions requiring long times, the gallium arsenide may be completely etched away. The arsenic content of the gallium phosphide crystals has not been determined; however, crystals with resistivities as high as 600 ohm-cm have been grown by this method, which indicates a high degree of purity by present standards. Since the growth process involves an open-tube arrangement, it is possible that the constituents of the gallium arsenide are carried away by the gas stream and do not enter into any further reactions. This is not the case for the Monsanto closed-tube technique, where reactant products remain in the system.

Conceptually, the Stanford University technique appears to be capable of producing gallium phosphide single crystals of purity and perfection exceeding that of any other known technique. Since additional crystals are not available from the University, the apparatus required to grow crystals by the Stanford University technique would have to be constructed if more crystals are needed. The details of the

Stanford apparatus are available so that this could be done if necessary. At present, it appears that the crystal on hand will be sufficient to complete the evaluation.

b. Crystal No. 2

Crystal No. 2, approximately 10 mm in diameter and 0.5 mm thick, was obtained from the Monsanto Chemical Company. This crystal represents the results of the latest techniques developed at Monsanto and is of the highest purity and resistivity currently available. This crystal contains up to two percent of arsenic, presumably due to the techniques used for its growth. It appears that as many of these crystals as desired will be available from Monsanto; however, the cost is fairly high ($240 per crystal). It is also possible to obtain crystals containing lower concentrations of arsenic, but the cost rises very rapidly as the arsenic content is lowered; the practical lower limit of arsenic is not known at present.

The complete details of the Monsanto process for producing gallium phosphide crystals have not been released; however, a limited amount of information has been obtained. Apparently, the Monsanto process involves a closed tube reaction, using iodine vapor to transfer the gallium phosphide constituents from a polycrystalline source to a seed wafer of gallium arsenide. This results in a gallium phosphide layer that contains about 15 percent arsenic. By lapping the arsenide substrate off and using the gallium phosphide layer as a substrate in a second deposition, a subsequent gallium phosphide layer containing only about two percent arsenic is obtained. The highest resistivity that has been obtained by this method is about 0.08 ohm-cm. It may be possible to perform more lapping and redeposition steps and improve the purity of the gallium phosphide further, but this has not been tried.

It is expected that the arsenic would substitute for the phosphorus in the gallium phosphide lattice and that the resulting crystal would exhibit the characteristics of a gallium-arsenide-phosphide alloy. The major effect to be considered would be the anticipated change

in the band gap; however, since the arsenic concentration is low, this change should be negligible.

c. Measurements

Hall effect, conductivity, and optical transmission measurements have been made on Crystals Nos. 1 and 2 to determine the important properties. A summary of these data and other characteristics is shown in Table I.

Table I

SUMMARY OF GALLIUM PHOSPHIDE PROPERTIES

	Crystal No. 1	Crystal No. 2
Conductivity Type	n	n
Impurity Type	Sulfur	Tellurium
Crystal Plane Exposed	[111]	[111]
Resistivity--ohm-cm	0.38	0.079
Hall Mobility--cm^2/volt-sec	125	110
Carrier Concentration--cm^{-3}	1.3×10^{17}	7.2×10^{17}
Band Gap--ev	2.15-2.22	2.15-2.22

(1) Hall Effect and Resistivity Measurements

Hall effect and resistivity measurements were made using the method of van der Pauw[25] and the measuring circuit of Dauphinee and Mooser.[26] Metallic lead was alloyed to the crystal to provide ohmic contacts. The measurements on Crystal No. 2 agree closely with those made by the supplier, Monsanto Co. The identity of the sulfur impurity and a rough estimate of the resistivity of Crystal No. 1 was the only information known about this crystal.

Mobilities in the range of 100-110 for low-resistivity gallium phosphide have been reported fairly consistently by other workers. The mobility of Crystal No. 1 is somewhat greater than this indicating that this crystal may have better crystalline structure than crystals produced by other techniques, or that impurity

scattering may be important at room temperature. If the latter is true, higher-resistivity gallium phosphide could be expected to have higher mobilities.

(2) Optical Transmission Measurements

Transmission-vs.-wavelength data have been obtained on both crystals using the Perkin Elmer spectrometer and the tungsten source as set up previously for photo-excitation tests on cathodes. While this measurement is not the most sensitive to changes in crystal constitution, it is the least involved method from which a reasonable amount of information can be obtained. Figure 2 shows the relative absorption for Crystal No. 1, and Fig. 3 shows the same data for Crystal No. 2. The interpretation of Figs. 2 and 3 follows below.

Electronic transitions across the band gap of gallium phosphide must involve the absorption or emission of a phonon in order to conserve crystal momentum. For this situation the absorption constant is related to the absorbed photon energy as

$$\alpha = C\left\{\frac{(E_p + E_s - E_g)^2}{\exp(E_s/kT) - 1} + \frac{(E_p - E_s - E_g)^2}{1 - \exp(E_s/kT)}\right\} \qquad (1)$$

$$= \alpha_+ + \alpha_-$$

where

E_p is the photon energy,

E_s is the energy of the phonon involved in the transition,

E_g is the forbidden band gap,

k is Boltzmann's constant,

T is the temperature in degrees Kelvin,

C is a constant, and

α is the absorption coefficient.

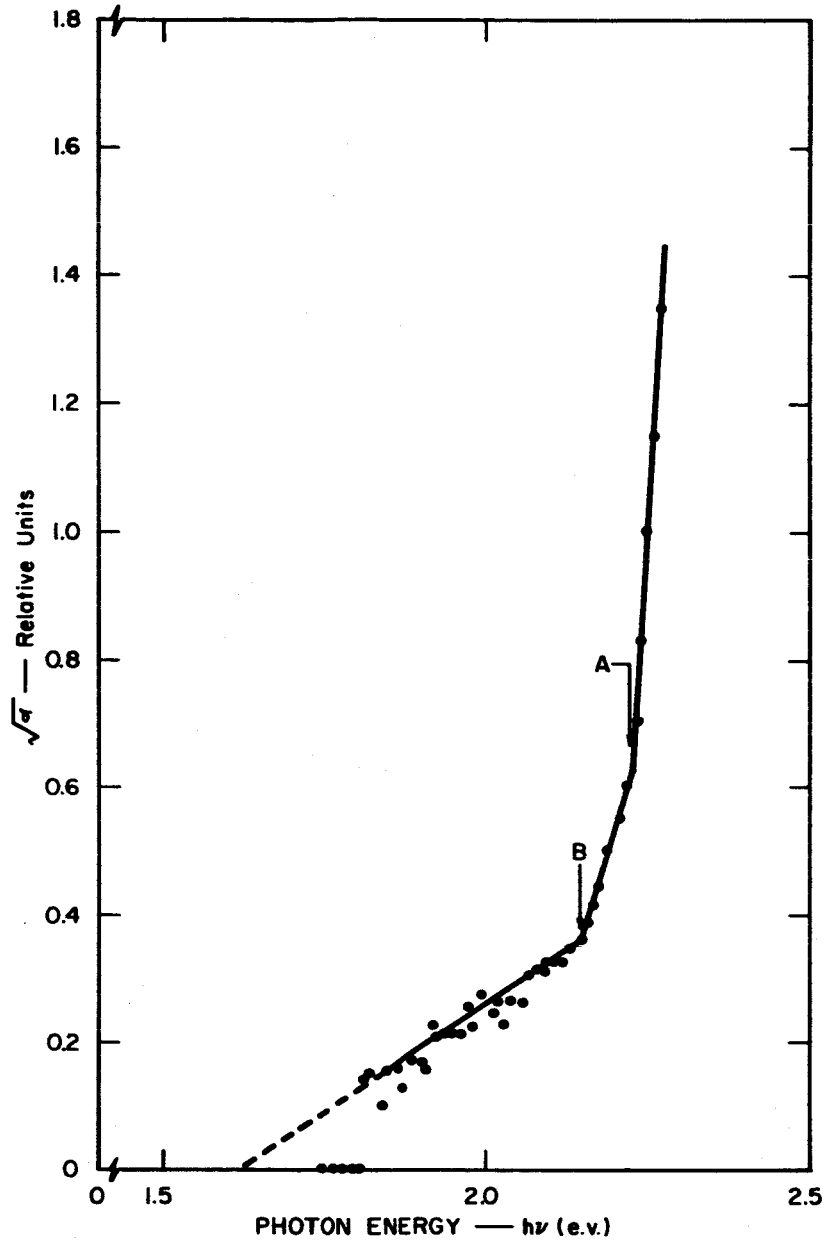

FIG. 2 RELATIVE ABSORPTION OF STANFORD GaP

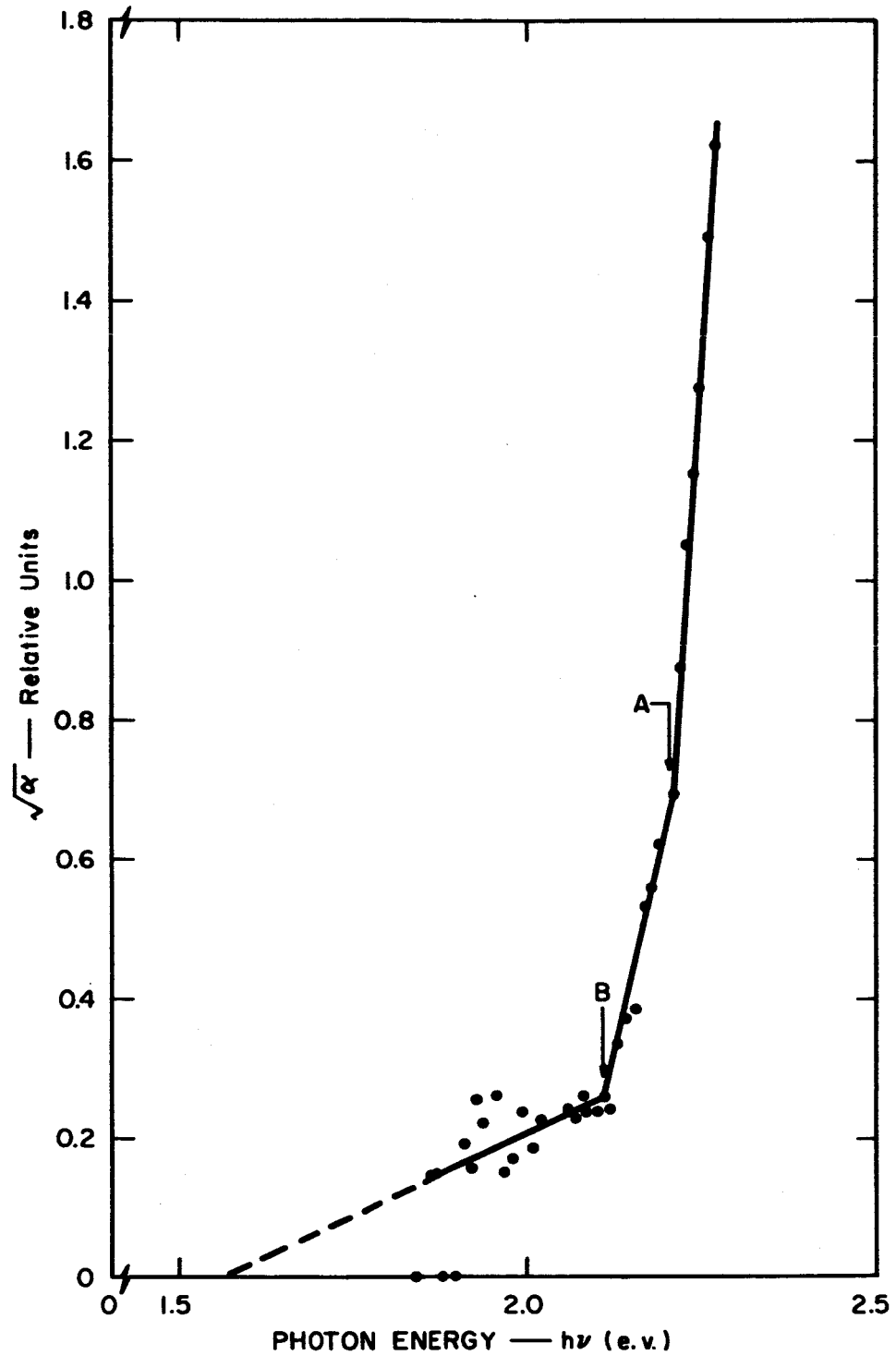

FIG. 3 RELATIVE ABSORPTION OF GaP SINGLE CRYSTAL NO. 2

The first term in the above equation can be considered as optical absorption resulting in the simultaneous absorption of a phonon (α_+), and the second term can be considered as the optical absorption resulting from the emission of a phonon (α_-). If more than one phonon is involved, additional terms must be added. From the experimental data, the two components of the absorption can be separated; and the strength of the phonons and the band gap of the material can be determined from the relationships:

$$E_g = \frac{1}{2}(E_+ + E_-) \qquad (2)$$

$$E_s = \frac{1}{2}(E_+ - E_-) \qquad (3)$$

where

E_+ is the $\alpha_+ = 0$ intercept, and

E_- is the $\alpha_- = 0$ intercept.

Figures 2 and 3 both show the effects of phonon absorption and emission; however, there is evidence that two prominent phonons are involved rather than only one. Presumably, breakpoint A on the curves is indicative of the effects of the higher-energy phonon, and breakpoint B indicates the effects of a lower-energy phonon. In order to separate the effects of these two phonons, an additional breakpoint should occur at a photon energy lower than breakpoint B. Since the data become badly scattered at low absorption coefficients, this breakpoint is not obvious and exact values of the band gap are not determinable. From the data obtained, it appears that the band gap should lie between 2.15 and 2.22 ev for both the Monsanto and Stanford crystals at the temperature of the measurements.

d. Surface Preparation

Lapping and polishing operations on gallium phosphide are accompanied by the release of phosphine gas. This is associated with any mechanical abrading process, which apparently enhances the formation of poisonous phosphorus compounds through catalytic action. Phosphine

gas is very high in toxicity, and the maximum allowable concentration is 0.05 ppm. Concentrations well below the maximum are easily detected as phosphine has a strong characteristic odor which becomes noticeable at very low concentration levels. Because of the toxic qualities of the lapping and polishing products, all mechanical operations should be done in a fume hood with a flow rate sufficient to maintain concentrations below the maximum allowable values.

A program was undertaken to optimize the surface preparation of GaP to be used as a substrate for metal depositions and barrier studies. This application requires a uniform mirror finish surface with very few, if any, etch or polish pits. It was found that one side of Crystal No. 1 did not polish as well as the other when subjected to mechanical lapping and polishing. This observation was confirmed using several different polishing techniques.

Good surfaces on other types of crystals had previously been prepared using Dymo polishing compounds. These are abrasive pastes containing diamond particles. The pastes are diluted to proper consistency by adding an eythelene glycol solution. Several methods were tried using 6 micron paste on both a glass plate and Buehler polishing wheel followed by 1/2-micron paste on a polishing wheel and using several types of wheel surfaces including silk, nylon, and Buehler AB Microcloth. These procedures gave fair results along with some pitting, especially on the side of the crystal that had previously been the roughest surface. It was thought that the diamond may be too harsh on the crystals causing small pieces to break from the surface.

Alumina in a deionized water slurry was tried next. Five micron particles followed by 0.3 micron particles on various backing plates and cloths all gave similar results. Silk and nylon cloths gave fair polish but many small scratches were evident. Fine microcloth gave high gloss but severely rounded edges and had a tendency to produce an "orange peel"-like surface. In all cases, small pits were evident under medium power magnification.

Electronic-grade methyl alcohol was substituted for the deionized water in the slurry. It was theorized that phosphine, which is released, could be combining with the water and forming an acid which was etching the crystal and producing pits. Subsequently, this procedure was dropped as pits were not eliminated and it was learned that Monsanto Co. used deionized water with good results.

It was found that the silk and nylon polishing cloths were too hard and the nap on the microcloth was too high for effective polishing of GaP crystals. Other cloths were tested; the best compromise for a flat uniform mirror surface was obtained with Buehler AB Texmet polishing cloth backed by a glass plate. All lapping and polishing was done by hand in a well-ventilated fume hood to protect personnel from the toxic phosphine which is released in the mechanical processing.

All of the finishes produced mechanically were inferior to those obtained earlier using a hot aqua regia etch. Etching the face of the crystals which had a good mechanical polish produced rough surfaces. Through experimentation it was found that the "A" (gallium) side of the crystal will etch to a mirror finish in hot aqua regia but will pit and scratch very easily by mechanical abrasion, while the "B" (phosphorus) side takes a good mechanical polish and etches to a matt finish in hot aqua regia.

Other etches tried included different concentration ratios of hydrochloric to nitric acid, various combinations of hydrofluoric and nitric acid, and even a nonaqueous etch made by bubbling chlorine gas through methyl alcohol. The best etch was found to be aqua regia at 70°C.

e. Ohmic Contacts

Ohmic contacts to gallium phosphide have been made by alloying metallic lead to the back side of the crystal. The apparatus shown in Fig. 4 is used for this operation. It consists of a carbon-cloth strip heater (shown in Fig. 5) enclosed in a pyrex bell jar provided with gas inlets and outlets so that alloying may be done in a

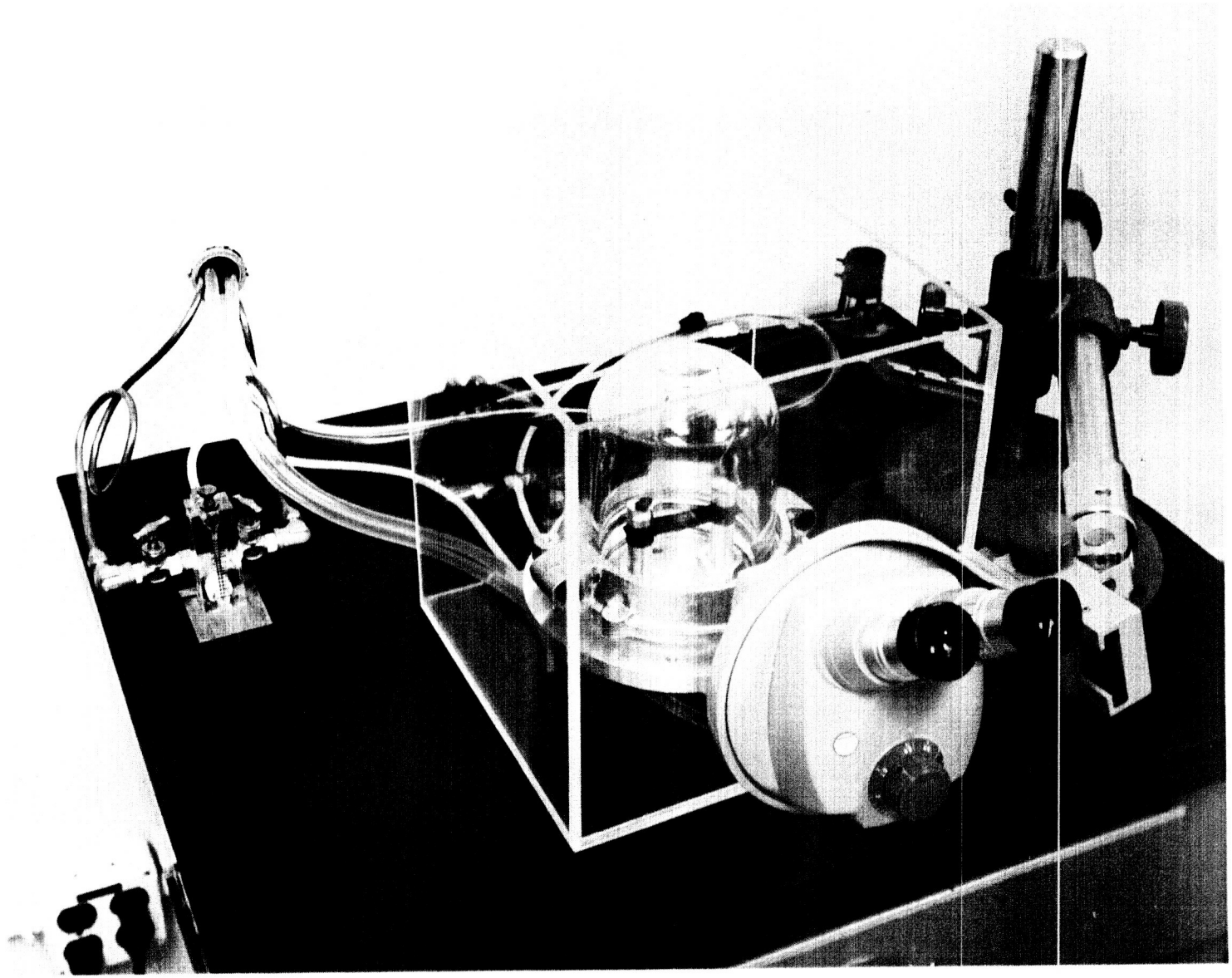

FIG. 4 ALLOYING STATION FOR OHMIC CONTACTS

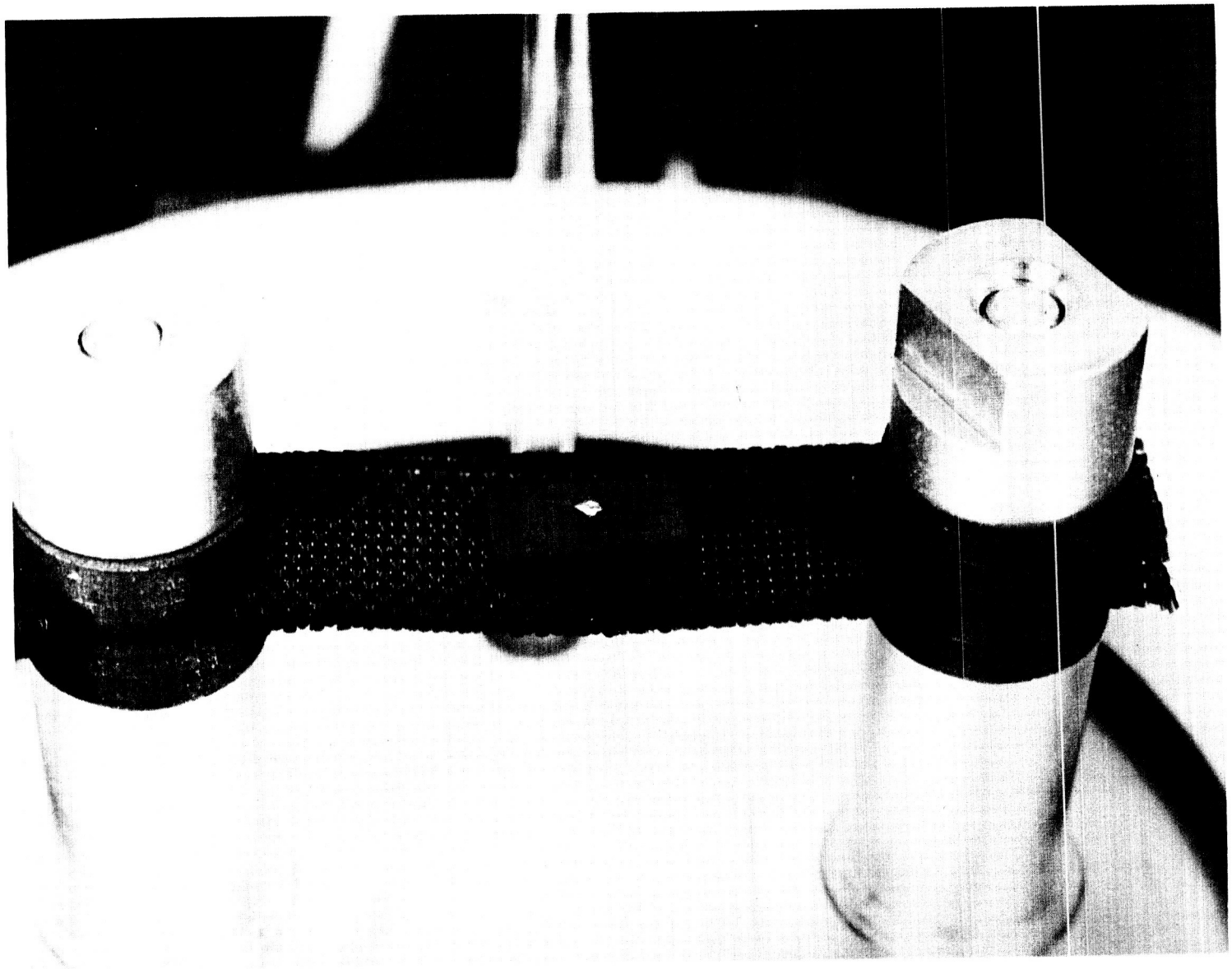

FIG. 5 CLOSE-UP VIEW OF GRAPHITE CLOTH-STRIP HEATER FOR ALLOYING STATION

controlled atmosphere. Purified and dried hydrogen was found to produce the most consistent results and seemed to act as an effective flux during the alloying operation. The small crystal on the purified graphite block resting on the carbon-cloth heater strip shown in Fig. 5 is in position for alloying. The heater strip temperature may be accurately controlled by means of a variable power supply (not shown). Current is supplied to the heater strip through the water-cooled supporting columns.

Metallic lead is a convenient material to use for laboratory contacts; however, a material with a higher melting temperature and higher vapor pressure is required for high vacuum devices. Silver containing one atomic percent tellurium makes a good ohmic contact to n-type gallium phosphide and has the required vacuum characteristics. Tellurium-doped silver was evaporated onto a gallium phosphide crystal and alloyed at about 900°C in the alloying station. To protect the silver from oxidation and from nitric acid etches used during other fabrication steps, a thin film of gold was evaporated over it. This provided a stable ohmic contact of the desired characteristics.

2. Blocking Contacts

As indicated previously, a high surface barrier is required between the semiconductor and the thin metal surface film. In order to be able to use evaporated BaO for the activator film, a barrier equal to or greater than about 1.3 ev is required. Of all the semiconductor/metal systems reported in the literature, only two semiconductors appear to meet the barrier height requirements: α-SiC and GaP.

a. Silicon Carbide

Some α-SiC crystals were given to us by Dr. D. Hamilton of Westinghouse. One of the crystals was polished and etched in molten NaCl. Small ohmic contacts were formed in four locations on one side of the crystal. These contacts were made with an alloy of gold and 15 percent tantalum by heating in a vacuum in steps to an ultimate temperature of 1570°C. Blocking contacts were applied to the other side of the crystal by evaporating platinum.

Figure 6 is a photograph of an I-V characteristic of the diode on a curve tracer. Because the barrier is obviously low, no attempt was made to measure a barrier height.

b. Gallium Phosphide

GaP-Pt Schottky diodes were fabricated by vacuum evaporation of Pt on GaP single crystals. On the first run the crystals were prepared by simple degreasing. The I-V characteristics of the resulting diodes possessed a suspiciously high forward break voltage, which was suggestive of a non-intimate metal-semiconductor contact (Fig. 7). On the next run, greater care was exercised in crystal preparation, with more meaningful results. The crystals were prepared by first etching in 50% HCl-50% H_2NO_3 for about three minutes. The crystals were not removed from the etchant. Instead, electronic-grade methyl alcohol was added until the concentration of the etchant was negligible. The crystal was placed in the vacuum chamber wet with alcohol, and the bell jar was evacuated as rapidly as possible. The purpose of this procedure was to minimize exposure to atmosphere and possible oxidation of the crystal.

At a pressure of about 10^{-6} torr, platinum was evaporated through an appropriate mask onto the GaP crystal. The platinum source was heated by electron-beam bombardment. No shuttering was used, and the vacuum system used an oil diffusion pump which was liquid-nitrogen trapped.

Lead was alloyed onto the other face of the crystals to form ohmic contacts. The I-V characteristics of two of the resulting diodes are shown in Figs. 8 and 9. These diodes were circular, having a diameter of 0.056 inch. Figure 10 is a semi-log plot of I vs. V, and Fig. 11 is a log-log plot for the same diode.

Capacitance-vs.-voltage data were taken on two of the 0.056 inch diameter diodes, and the resulting $1/C^2$-vs.-V plots are shown in Figs. 12 and 13. In Fig. 12, the extrapolation of the straight-line reverse characteristic yields an intercept of about 3.7 ev, which clearly cannot be the barrier height. The forward characteristic is beginning

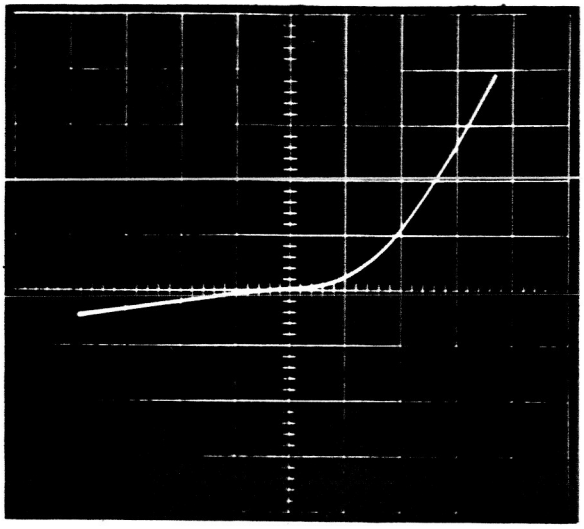

FIG. 6 I–V CHARACTERISTICS OF SiC–Pt DIODE
Horizontal scale: 1 volt/division
Vertical scale: 200 μa/division

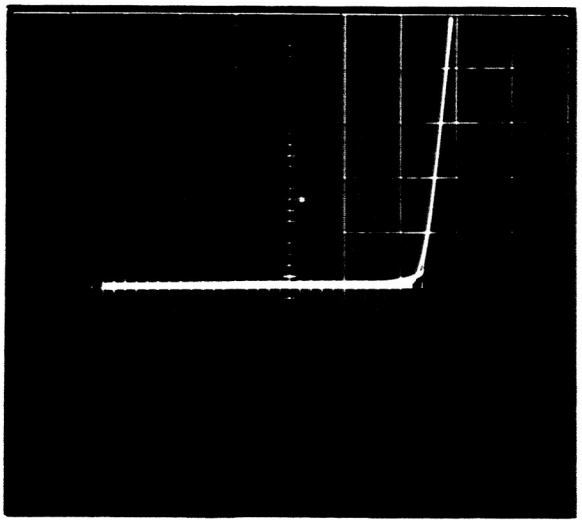

FIG. 7 I–V CHARACTERISTICS OF GaP–Pt DIODE
Horizontal scale: 1 volt/division
Vertical scale: 10 μa/division

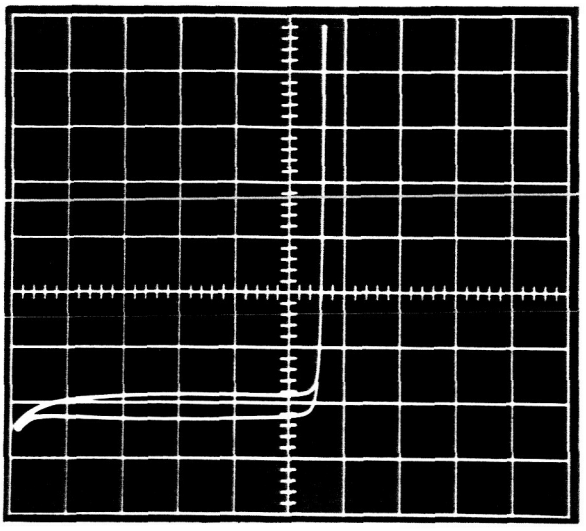

FIG. 8 I-V CHARACTERISTICS OF GaP-Pt DIODE
Horizontal scale: 5 volts/division
Vertical scale: 10 μa/division

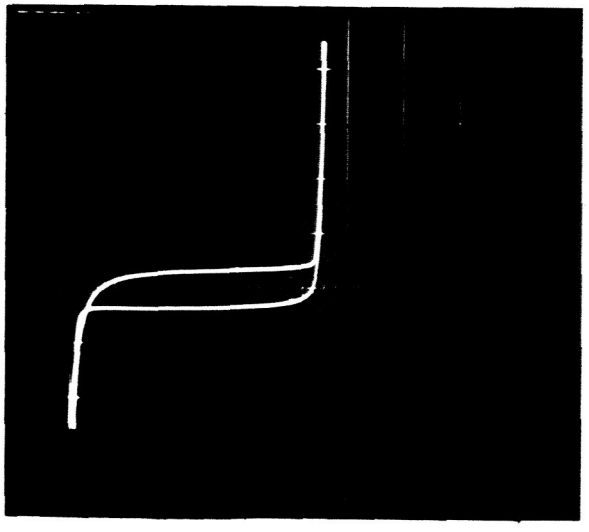

FIG. 9 CHARACTERISTICS OF GaP-Pt DIODE
Horizontal scale: 2 volts/division
Vertical scale: 10 μa/division

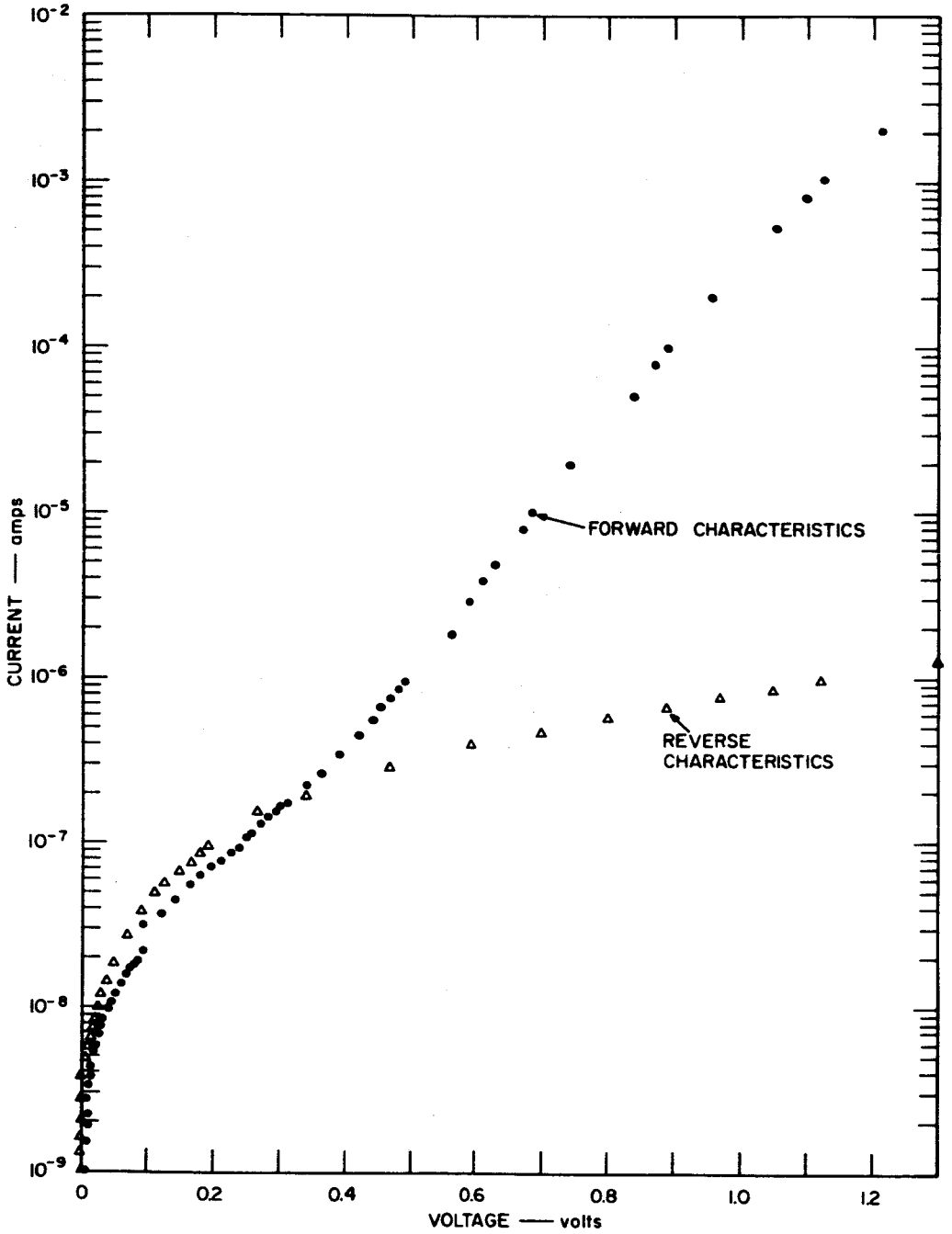

FIG. 10 CONDUCTION CHARACTERISTICS OF GaP–Pt DIODE

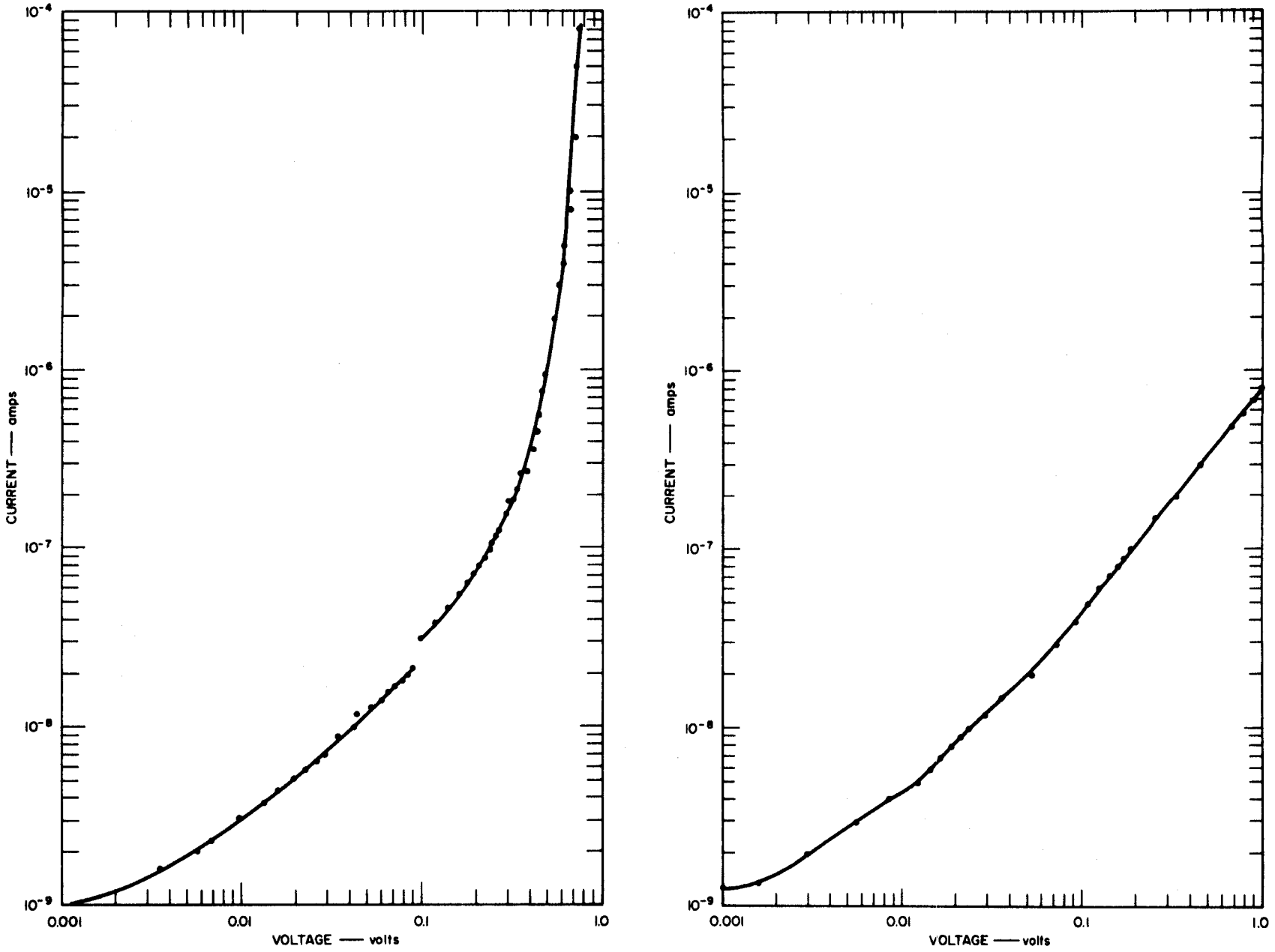

FIG. 11 I-V CHARACTERISTICS OF GaP-Pt DIODE

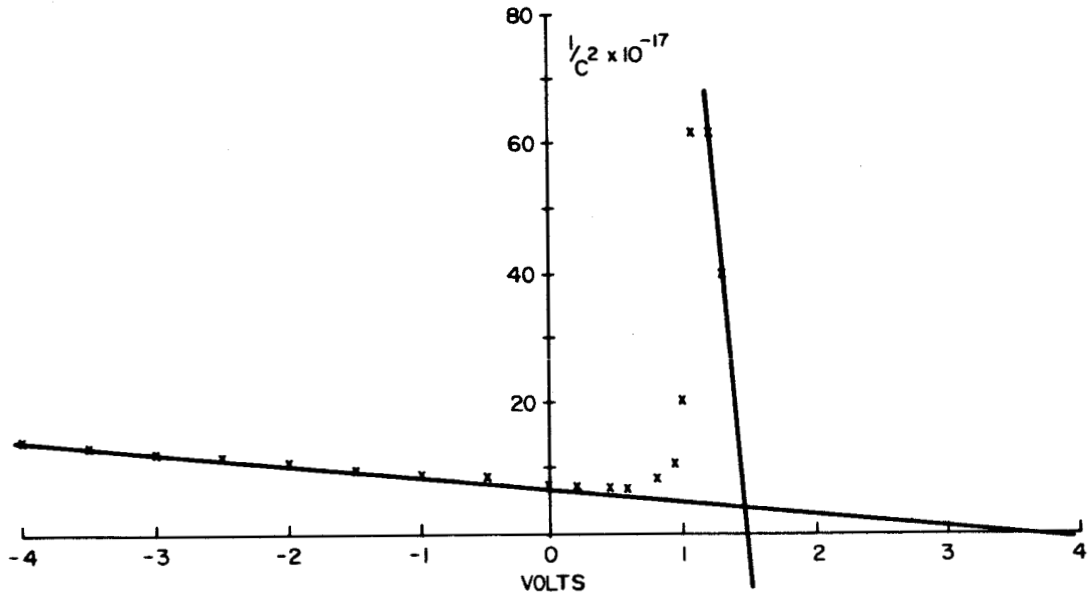

FIG. 12 $1/C^2$ vs. V PLOT FOR GaP–EVAPORATED Pt — DIODE 2

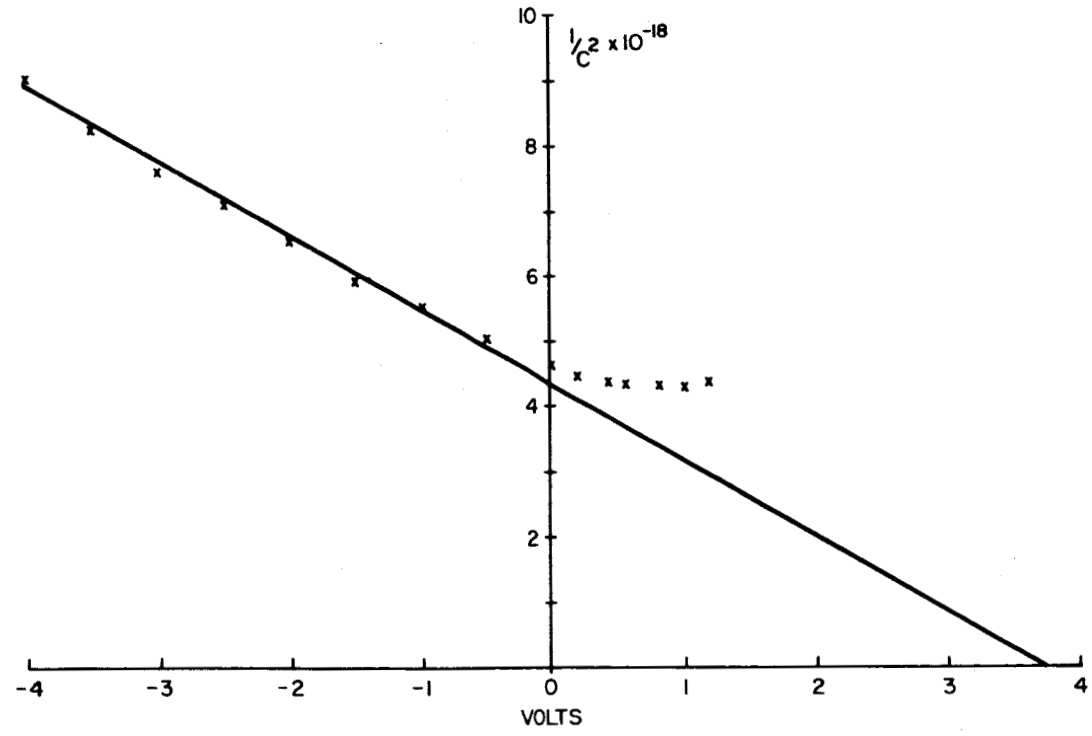

FIG. 13 $1/C^2$ vs. V PLOT FOR GaP–EVAPORATED Pt — DIODE 3

to drop at about 1.25 ev, however, indicating a barrier height of about 1.5 ev. In the case of the other diode, the curve could not be extended far enough in the forward direction to obtain a drop in $1/C^2$, so that no barrier height could be deduced, as shown in Fig. 13. In this case, extrapolation of the reverse-bias straight line portion yields an intercept of about 3.75 ev, which again is clearly too high to represent the barrier height. These results will be discussed shortly.

One of the diodes was then mounted on the PE112 spectrometer and a zero-bias spectral response was taken. Figure 14 is a Fowler plot of the square root of the response-vs.-photon energy, and the extrapolated intercept of the straight-line cutoff region indicates a Schottky barrier height of about 1.4 ev, in agreement with the $1/C^2$-vs.-V forward data of Fig. 12, and also in agreement with the results obtained by Cowley.[17] All of these data will now be discussed in detail.

The semi-log plot shown in Fig. 10 indicates that the forward current follows the law $I \propto \exp\left(\frac{qV}{nkt}\right)$ over the straight-line portion of the characteristic, where n is about 3.5. According to simple Schottky theory, n should be unity, so the barrier is not of the simple Schottky type.

Another indication that the barrier is not of the simple Schottky type is the large values of zero intercept obtained on the $1/C^2$-vs.-V plots of Figs. 12 and 13. It has been learned from Dr. A. M. Cowley* that similar results on $1/C^2$ vs. V were obtained on GaP-Pt diodes at Stanford University when the Pt was evaporated in an oil-diffusion-pumped system. When the Pt was evaporated in an ion-pumped system, on the other hand, low intercepts of about 1.45 ev were obtained; and this value checked well with barrier heights Cowley obtained from hot-electron data. Cowley attributes these results to a contaminating oil film in the case of the Pt evaporated in the oil-diffusion-pumped system.

---

*Personel communication.

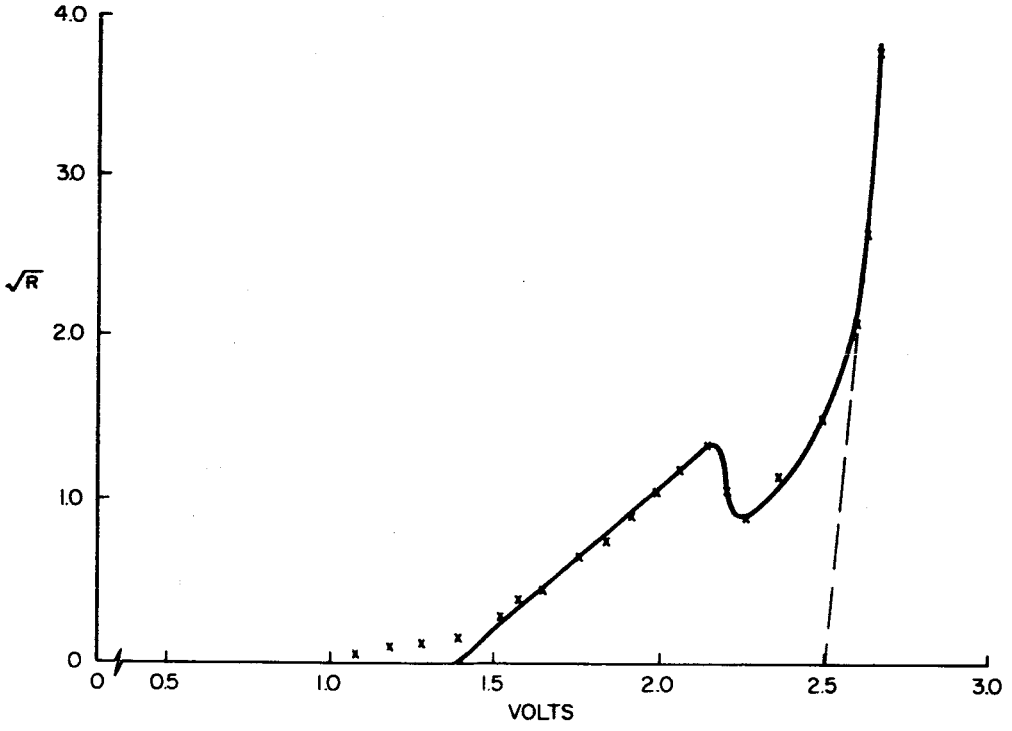

FIG. 14 FOWLER PLOT FOR GaP–EVAPORATED Pt

Such a contaminated interface might also explain the high value of $\underline{n}$ found from the slope of the log I-vs.-V plot of Fig. 10. In essence, the contaminated layer, which is in series with the true barrier, reduces the forward current well below the theoretical values corresponding to $\underline{n}$ unity.

Because there is a contaminating oil film between the GaP and the Pt, the $1/C^2$-vs.-V plot does not approach zero when the barrier is reduced to zero but instead approaches $1/C_1^2$, where $C_1 = \underline{A}\ \epsilon_f/t_f$ (ϵ_f = film permittivity, and t_f = film thickness). From Fig. 6, $1/C_1^2$ is seen to be approximately 4×10^{17} farad^{-2}, which implies a C_1 value of 1600 pf. For a dielectric constant of unity, this capacitance value corresponds to a film thickness of 60Å. This film thickness is reasonable for large organic molecules.

The slope of the $1/C^2$-vs.-V curve should still correspond to the donor density in the semiconductor, even when a contaminating film exists between the semiconductor and the metal. From the slope observed in Fig. 6, a donor density of 6.85×10^{17} cm^{-3} can be calculated. The measured resistivity is 0.079 ohm-cm for this GaP, and the measured mobility is 110 cm^2/volt^{-1} sec^{-1} (Table I). From these values a donor density of 7.0×10^{17} cm^{-3} can be calculated. This value is in good agreement with the 6.9×10^{17} cm^{-3} obtained from the capacitance measurements.

There is evidence of series resistance limiting the forward current at high values of forward bias. If the straight-line portion of the log I-vs.-V plot of Fig. 10 is extrapolated upwards and the voltage difference between this line and the experimental curve is plotted against the current, a straight line results with a slope corresponding to a series resistance of about 1000 ohms. The most likely explanation for this series resistance is the high resistance caused by the contamination at the interface.

The hot-electron technique for measuring barrier heights appears to be the most reliable method available, since the proper results are evidently obtained even for an unclean semiconductor/metal

junction. By the same token, however, the cleanliness or perfection of the interface cannot be ascertained by this method. It would appear to be desirable, therefore, to take $1/C^2$-vs.-V data as well as hot-electron data in order to obtain the maximum amount of information possible.

Still a third method of obtaining barrier heights is to use the Richardson equation,

$$J = AT^2 \exp\left(-\frac{q\Phi_b}{kT}\right)\left[\exp\left(\frac{qV}{kT}\right) - 1\right] \qquad (4)$$

where Φ_b is the barrier height and V is the applied voltage. This equation neglects image forces, so that it should be applied only for low voltages and currents. A small error is introduced because of the uncertainty in A. An attempt was made to calculate Φ_b from this equation, using the experimental data of Fig. 10 and the vacuum emission for A of 120 amp/cm^2 deg K^2. The current was chosen at 0.1 volt bias to minimize the effects of image force lowering of the barrier. The result was a Φ_b of about 0.7 ev. This is too low and probably results from a leakage condition. This particular diode had been made a month previous to taking the data in Fig. 10, so there may have been some contamination. The forward-bias data cannot be used reliably because of the high value of n in $\exp\frac{qV}{nkT}$ compared to unity. When simple Schottky theory can be made to apply ($n \cong 1$), the value of Φ_b obtained from the Richardson equation should check well with the values obtained from $1/C^2$-vs.-V and from hot-electron data.

A GaP-Pt diode has been on dynamic life test for over 1000 hours with no significant changes in characteristics. Figure 15 is a photograph of the I-V characteristics of this diode as displayed on a curve tracer.

A considerable amount of effort has been expended in attempting to develop a quantitative theory that will enable accurate prediction of metal/semiconductor surface barrier heights. A paper has

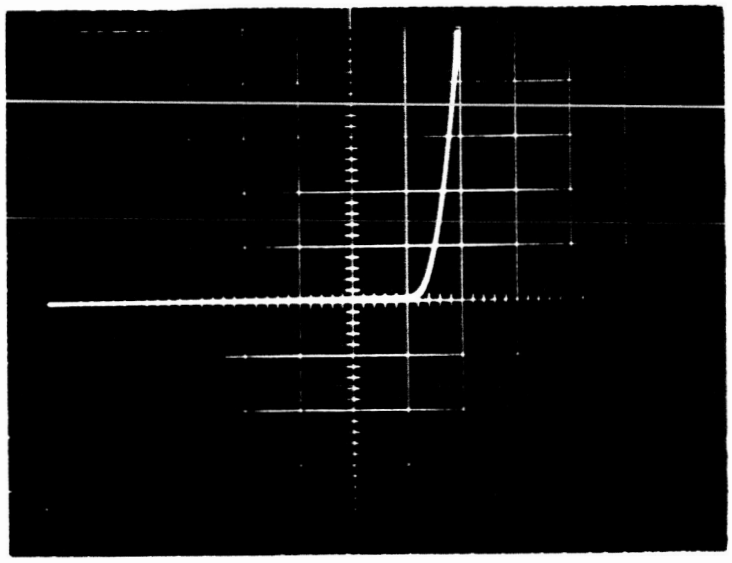

FIG. 15 PHOTOGRAPH OF I-V CHARACTERISTICS OF GaP/EVAPORATED Pt-DIODE ON LIFE TESTER
Horizontal Scale: 1 volt/div.
Vertical Scale: 200 μa/div.

been prepared recently concerning an attempt to verify Schottky theory; Appendices B and C comprise a preprint of this paper.

C. ACTIVATION

The approach in this study has been based largely upon the results obtained by Moore and Allison[5] in activating various metals with thin evaporated films of BaO. They reported thermionic work functions as low as 1.0 ev with BaO on various refractory metals. A number of photoelectric experiments has been performed, and the results are promising.

In these experiments the BaO was derived from a $BaCO_3$ deposit that was converted to the oxide. A shutter was incorporated in the phototube to shield the substrate during the conversion. In initial experiments with Mo the cathode was a piece of sheet Mo. In later experiments the metal was evaporated onto a substrate just before the activation began.

A heater was incorporated in the substrate to liberate any free Ba that may have been deposited in evaporating the BaO. The photoresponse was measured with a PE112 spectrometer using a W source. In most cases the phototubes were gettered with Ba and tipped off to make this measurement. The tubes with evaporated Pt cathodes were tested on the pumping station by bringing the vacuum system up to the spectrometer and by using a lens system to focus the light.

The objective with the last two tubes made was to determine the lowest attainable work function with BaO on evaporated Pt. In tube No. 5 the Pt source burned out before the Ta substrate was uniformly covered with Pt, so the results were somewhat ambiguous (Fig. 16). The lower intercept of 1.32 ev is attributed to the Ta. The Pt source in tube No. 6 was heated by induction so a satisfactory film was deposited on a Mo substrate, resulting in a work function of about 1.6 ev (Fig. 17).

Figure 18 is a plot of the square root of the response-vs.-photon energy from the most recent measurements made on phototube No. 4, a Ag-BaO tube. This is the type of plot that has been made in analyzing all the data obtained, and in the literature is often referred to as a "Fowler Plot." A review of the early literature in this area (e.g., Hughes and DuBridge[27]) discloses that the term "Fowler Plot" originally referred to a plot of $\log_{10} (I/T^2)$ vs. $h\nu/kT$. A comparison of these two types of analyses is made in Appendix A; and Fig. 19 is a plot of the latter type, using the same data from phototube No. 4.

The results obtained from the two methods in this case are identical. The main difficulty with the $\sqrt{R}$-vs.-$h\nu$ plot is in determining accurately the location of the intercept when the response near threshold departs somewhat from a square-law dependence on energy. Through use of the more rigorous log plot it is usually possible to overcome this difficulty.

An off-axis ellipsoidal mirror has been mounted at the exit slit of the spectrometer. It produces a demagnified image of the exit slit approximately 0.100 in X 0.025 in. This attachment will facilitate future measurements of barrier heights and work functions on small structures.

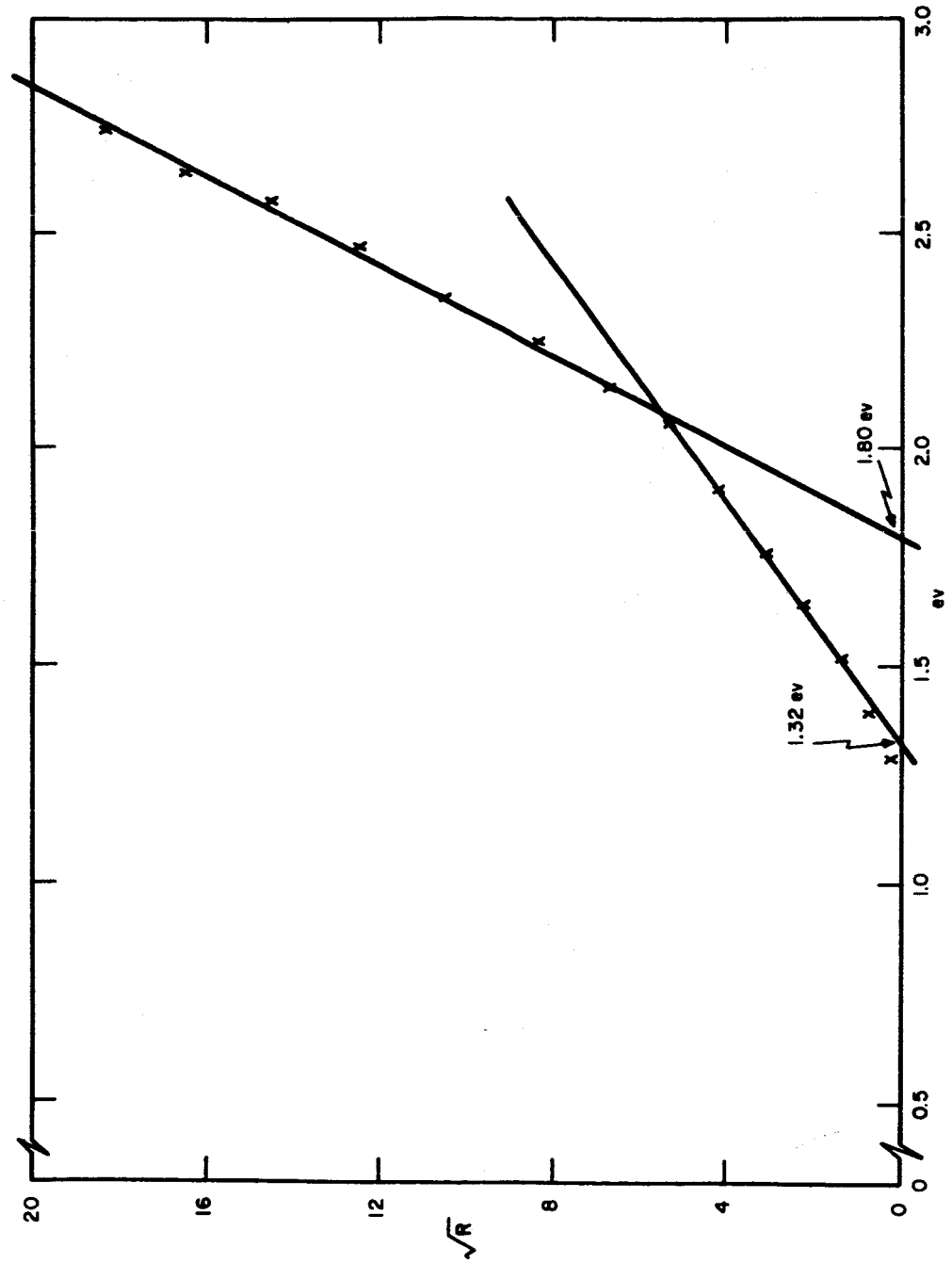

FIG. 16 SQUARE-ROOT OF PHOTORESPONSE vs. PHOTON ENERGY FOR Ta-Pt-BaO PHOTOTUBE

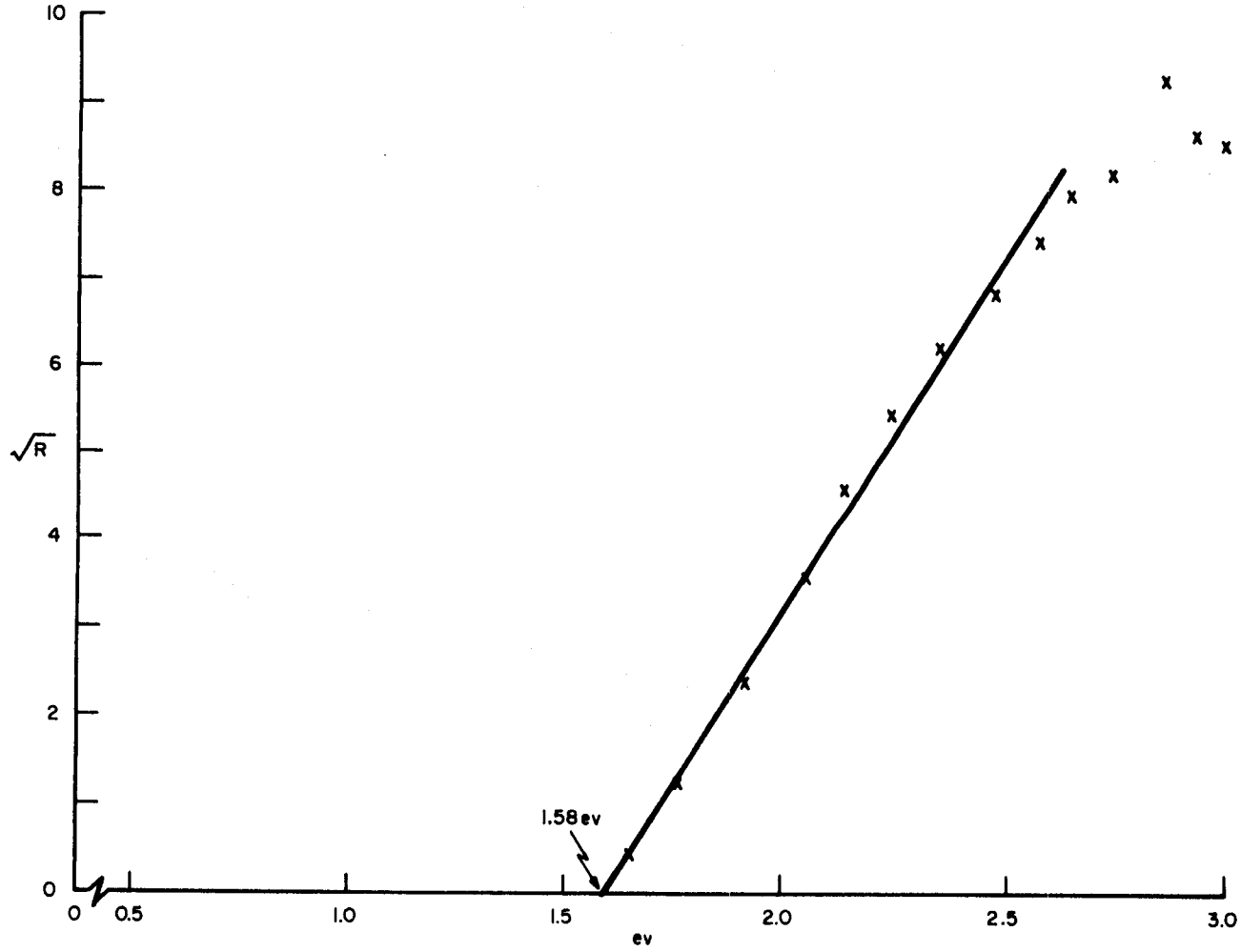

FIG. 17 SQUARE-ROOT OF PHOTORESPONSE vs. PHOTON ENERGY FOR Pt-BaO PHOTOTUBE

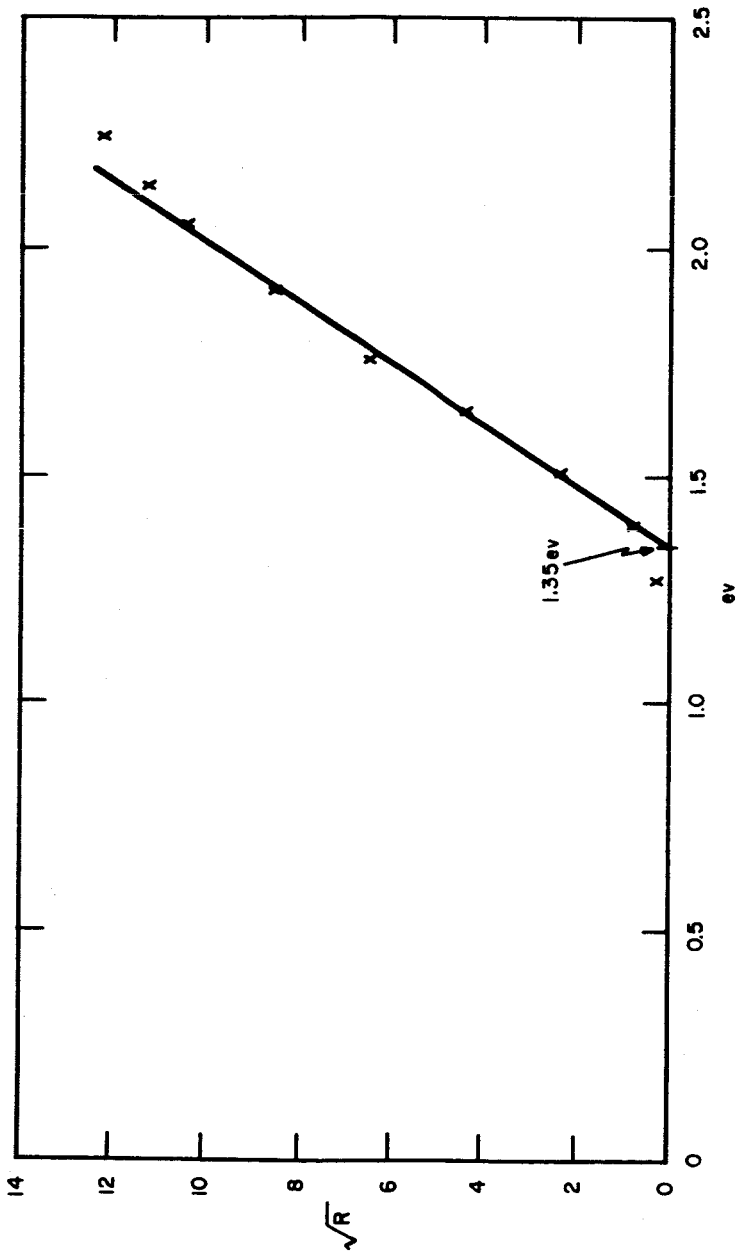

FIG. 18 SQUARE-ROOT OF PHOTORESPONSE vs. PHOTON ENERGY FOR Ag-BaO PHOTOTUBE AFTER NINE MONTHS

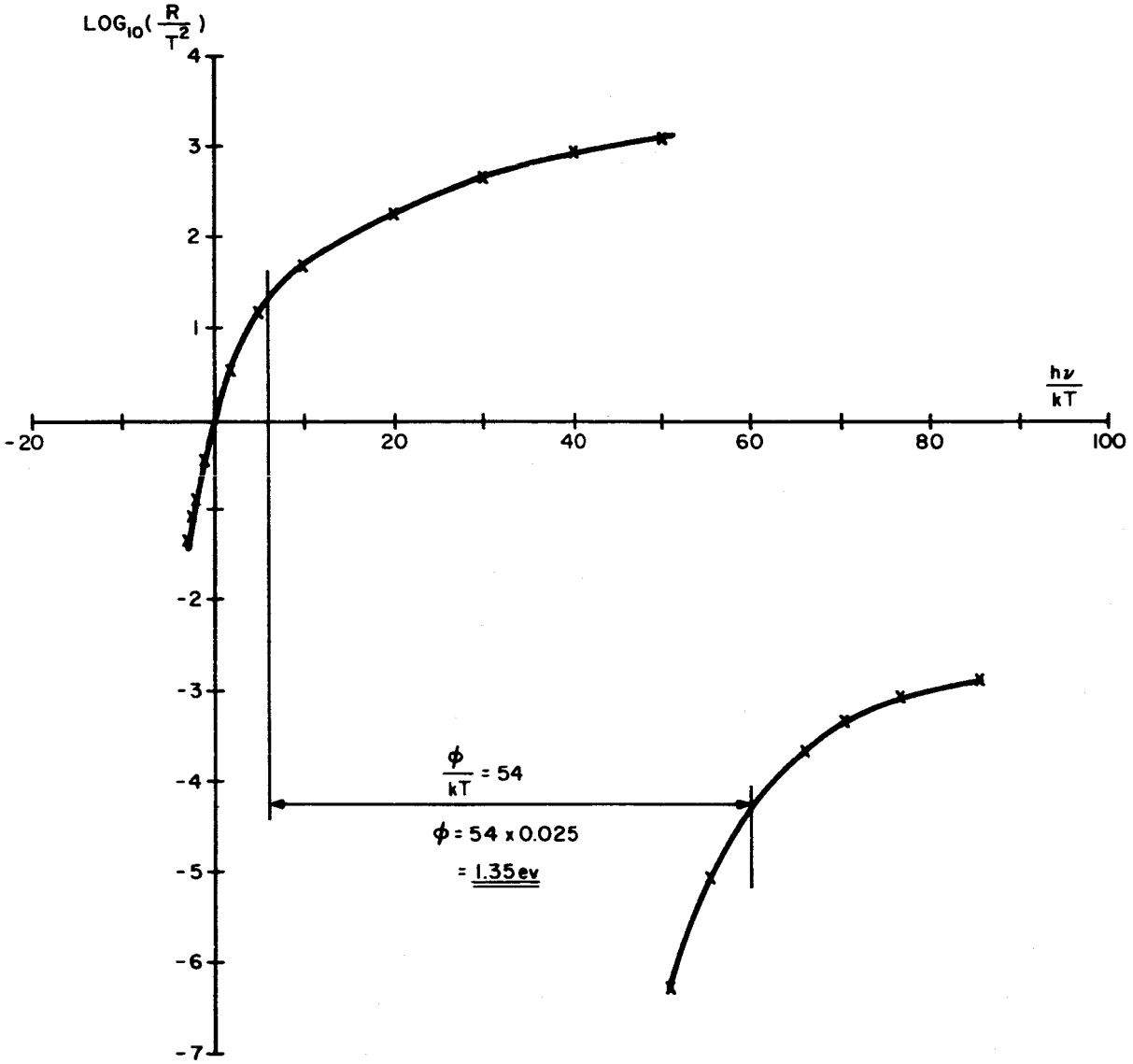

FIG. 19 FOWLER PLOT FOR Ag–BaO PHOTOTUBE AFTER NINE MONTHS

From the experimental results, it appears unlikely that vacuum barriers below 1.5 ev can be obtained with BaO on evaporated Pt. Moore and Allison[5] did not measure BaO on Pt but they report a value of 1.9 ev for SrO on Pt. Since they obtained almost identical values for BaO and SrO on Mo, W, and Ta, the values above 1.5 ev for BaO on Pt are not unreasonable. The measured height of the Schottky barrier formed by GaP and Pt is less than 1.5 ev; it will therefore be necessary to use another metal or a combination of metals. Since Ag and Ta have been activated to values below 1.5 ev with BaO, a thin film of Pt could be used next to the GaP to obtain the necessary Schottky barrier, followed by a thin film of Ag or Ta which would be treated with BaO in the usual manner.

Another possibility is to replace the Pt with another metal having a slightly lower work function. Experiments are being conducted on W films; and if Schottky barriers on the order of 1.3 ev can be obtained, it might be a suitable replacement for Pt. Ni is another metal that is being considered for this purpose.

When a metal is activated with a low work function element like Cs, the reduction in the work function of the metal can be explained in terms of a dipole layer on the surface. The Cs is absorbed as positive ions with an opposing negative charge on the surface of the metal. The reduction in work function is

$$\Delta\varphi = 4\pi Ne^2 d \quad , \qquad (5)$$

where N is the number of absorbed ions per cm^2 and d is the distance between the positive and negative charges.

If a similar model can be applied to the BaO activation process, then the final value of φ would be related to the work function of the metal, φ_m. However, Moore and Allison[5] point out that the cleanliness of the metal surface has a dominating effect. Uniformly low values of φ were obtained with the refractory metals Mo, W, and Ta which were thoroughly outgassed by prolonged heating. On the other hand, their Pt and Ni substrates could not be heated to the same extent and did not activate as well.

With evaporated metal films, optimum activation with BaO can be obtained if the films are evaporated in a vacuum that precludes any gas absorption on the surface before the BaO activation is started. From the results obtained in this laboratory, the rate at which the BaO is evaporated also seems to be important. Moore and Allison[5] claim that free Ba has no appreciable effect, but it has been observed that a rapid evaporation usually results in higher barriers than with slower evaporations. This effect can be largely overcome by heating the substrate to liberate the free Ba produced by the higher source temperatures.

The results obtained with BaO-Ag phototube No. 4 are very encouraging. The most recent measurement of 1.35 ev was made nine months after the initial measurement of 1.44 ev. This indicates that BaO-activated cathodes will not deteriorate over extended periods of time in a good vacuum. The actual pressure in this barium-gettered tube cannot be determined, but it is assumed to be on the order of 10^{-9} torr. The fact that the latest value of φ is lower than the previous values does not necessarily mean that the tube has improved with time. The cathode area in this tube is large and there is some variation in the amount of activation over this surface. The value of 1.35 ev was obtained by maximizing the response on the spectrometer as the light was focussed on different areas.

III CONCLUSIONS AND SUMMARY

GaP appears to be an excellent choice for the semiconductor to use in the surface-barrier cold cathode. Good-quality crystals are obtainable from Monsanto Chemical Co. Techniques have been developed in our laboratory for surface preparation of the crystals. Good ohmic contacts have been demonstrated with Pb and with alloyed Te-doped Ag. Good blocking contacts have been obtained with evaporated Pt. Long life and stability have been demonstrated for GaP-Pt diodes on dynamic life test.

Direct use of a GaP-Pt, cold-cathode emitter does not appear to be possible, however, because BaO-activated platinum has a higher work function ($\sim$ 1.55 ev) than the GaP-Pt surface barrier ($\sim$ 1.45 ev). One solution to this problem would be to evaporate a double metal layer onto the GaP, e.g., Pt followed by Ag. The Pt would then form a high surface barrier ($\sim$ 1.45 ev) and the Ag would activate well with BaO to form a low vacuum work function ($\sim$ 1.35 ev). A more desirable solution, however, would be to find some single metal, M, such that GaP-M-BaO would form a workable combination.

Long life and stability for low-work-function evaporated BaO surfaces have been demonstrated in an ultra-high vacuum environment. The theory of metal/semiconductor contacts has been extended and refined.

IV PROGRAM FOR NEXT INTERVAL

1. Fabricate and test GaP-W surface barrier diodes.
2. Fabricate and test W-BaO phototubes.
3. If the system GaP-W-BaO looks worthwhile, fabricate and test a surface barrier cold cathode using this combination of materials.
4. Continue life tests on GaP-Pt diode and on BaO phototubes.

APPENDIX A

PHOTOELECTRIC THRESHOLD MEASUREMENTS FOR METAL SURFACES AND METAL-SEMICONDUCTOR SURFACE BARRIER JUNCTIONS

APPENDIX A

PHOTOELECTRIC THRESHOLD MEASUREMENTS FOR METAL SURFACES AND METAL-SEMICONDUCTOR SURFACE BARRIER JUNCTIONS

The emission of photoelectrons over the barrier at the interface of a metal-semiconductor contact is completely analogous to the well-known vacuum photoelectric effect, and just as the vacuum photoelectric effect has been used to determine the work function φ_m of solids, especially metals, the photo-effect in surface barrier junctions can be used to measure the barrier height φ_b. This appendix briefly outlines the theory of the photo-effect according to Fowler[28] and shows the equivalence of the Fowler method to the commonly used "square-root yield vs. $h\upsilon$" method [c.f for example, C. R. Crowell, et al., Phys. Rev. 127, p. 2006 (1962)].[11]

FOWLER THEORY

The Fowler Theory of the photoelectric effect is based on the Sommerfeld free-electron theory of a metal. It is well established, of course, that the Sommerfeld model gives only a very crude picture of the electron distribution in most metals. However, for the purpose of calculating the photoemission for photon energies which are only slightly greater than threshold, it turns out that the Sommerfeld model gives a theoretical expression for the photoelectric yield-vs.-photon energy which is in good agreement with experiment for most metals.

The Sommerfeld model treats the metal as a potential well, with a potential step, at the surface, as shown in Fig. A1. The height of the potential step at the surface, measured from the Fermi level, may represent the work function φ_m in the case of the metal-vacuum interface, or the barrier height φ_b, in the case of a metal-semiconductor contact. In any case, this quantity will be denoted by the symbol φ.

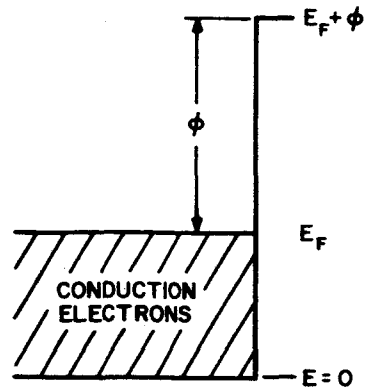

FIG. A-1 ENERGY DIAGRAM OF METAL SURFACE (Sommerfeld Model)

The relative photoelectric yield in electrons/photon can be calculated by first considering the distribution function N(E) for the flux of electrons having energy E directed perpendicular to the emitting surface of the metal. Fowler[29] derives N(E) from straightforward statistical considerations as

$$N(E) = \frac{4\pi mkT}{h^3} \log_e \left[1 + \exp\left(\frac{E_F - E}{kT}\right)\right] \qquad \text{(A-1)}$$

where E_F is the Fermi energy.

The following assumptions* are made regarding the interaction of photons with the assembly of electrons in the metal:

(1) A photon with energy $h\nu$ imparts all of its energy to the electron in a direction perpendicular to the surface, i.e., the perpendicular energy of an electron with initial perpendicular energy E is $E + h\nu$ after the interaction.

(2) The probability of an electron absorbing a photon is independent of its energy.

---

*A discussion of these and other assumptions is given by L. A. DuBridge.[30]

These two assumptions are equivalent to stating that when a stream of photons illuminates a metal, a small fixed fraction K of the electrons in each energy increment dE are shifted upward in energy by the photon energy $h\nu$. Denoting the "shifted" distribution by N′ we can write

$$N'(E) = K \frac{4\pi mkT}{h^3} \log_e \left[1 + \exp\left(\frac{E_F - E + h\nu}{kT}\right)\right] \quad . \qquad \text{(A-2)}$$

Integration of N′(E) over all energies greater than the potential step* yields the photoelectric current per unit photon flux, or the photoelectric yield, as it is commonly called:

$$Y(h\nu) = K \frac{4\pi mkT}{h^3} \int_{E_F+\varphi}^{\infty} \log_e \left[1 + \exp\left(\frac{E_F - E + h\nu}{kT}\right)\right] dE \quad . \text{(A-3)}$$

Changing the variable allows this integral to be written

$$Y(h\nu) = K \frac{4\pi mkT}{h^3} \int_{0}^{\infty} \log_e \left[1 + \exp\left(\frac{[h\nu - \varphi] - E'}{kT}\right)\right] dE' \quad . \text{(A-4)}$$

The integral in (A-4) has been evaluated as an infinite series by Fowler[28] and can be written

$$Y(h\nu) = K \frac{4\pi m(kT)^2}{h^3} \left[\frac{\pi}{6} + \frac{1}{2} u^2 - \left\{e^{-u} - \frac{e^{-2u}}{2^2} + \frac{e^{-3u}}{3^2} - \ldots\right\}\right]$$

$$(u \geq 0) \qquad \text{(A-5)}$$

where $u = \frac{h\nu - \varphi}{kT}$.

When T = 0, Eq. (A-5) reduces to

$$Y(h\nu) \xrightarrow[T=0]{} \frac{2K\pi m}{h^3} (h\nu - \varphi)^2 \quad . \qquad \text{(A-6)}$$

---

*This is tantamount to assuming that the transmission coefficient of electrons over the barrier is unity if $E > \varphi + E_F$ and zero if $E < \varphi + E_F$. This point is also discussed by DuBridge (op.cit.).[30]

For $u \gg 1$, i.e., $h\nu \gtrsim \varphi + 3kT$, a good approximation to Eq. (A-5) is

$$Y(h\nu) \approx \frac{2K\pi m}{h^3} (h\nu - \varphi)^2 \qquad \text{(A-7)}$$

i.e., for photon energies such that $h\nu \gtrsim \varphi + 3kT$, the yield is well approximated by its zero temperature value. It is thus expected that for photon energies more than 3kT or so above the threshold the yield will vary as the square of photon energy. If the square root of the measured response is plotted, a straight line should result which, when extrapolated to the Y = 0 axis, yields the work function or barrier height φ. This is the method used by Crowell et al. (op. cit.).[11]

Equation (A-5) may be divided by T^2 and rewritten as follows:

$$\frac{Y(h\nu)}{T^2} = C\, f(u) \qquad \text{(A-8)}$$

where $C = K \frac{4\pi mk^2}{h^3}$ and $f(u) = \frac{\pi^2}{6} + \frac{1}{2} u^2 - \left\{ e^{-u} - \frac{e^{-2u}}{2^2} + \frac{e^{-3u}}{3^2} - \ldots \right\}$.

Taking the common logarithm of Eq. (A-8) we obtain

$$\log_{10} \left[\frac{Y(h\nu)}{T^2} \right] = \log_{10} [C\, f(u)] = B + F(u) \qquad \text{(A-9)}$$

where $F(u) = \log_{10} f(u)$.

F(u) is a universal curve which has been calculated and tabulated [c.f. A. L. Hughes and L. A. DuBridge[27]]. Evidently a plot of experimental values of $\log_{10}(Y/T^2)$ vs. $h\nu/kT$ will yield a curve which is displaced B units vertically and φ/kT units horizontally from a plot of the universal curve F(u). The amount of horizontal displacement yields the barrier height φ in units of kT, at any temperature. This is the method originally used by Fowler.

The two methods just described are evidently equivalent if sufficient data with $h\nu \geq \varphi + 3kT$ can be obtained for the "square root" method. The "$\log \left(\frac{Y}{T^2}\right)$" method is preferable if reliable data can be obtained only within a few tenths of an ev of threshold. Figures 18 and 19, Sec. II-C, provide a comparison of the two methods for the case of a BaO-activated Ag photocathode.

APPENDIX B

CORRELATION OF METAL-SEMICONDUCTOR BARRIER HEIGHT AND METAL WORK FUNCTION; EFFECTS OF SURFACE STATES

APPENDIX B

CORRELATION OF METAL-SEMICONDUCTOR BARRIER HEIGHT AND METAL WORK FUNCTION; EFFECTS OF SURFACE STATES

1. Introduction

The height, φ_b, of a metal-semiconductor surface barrier, as given by the Schottky theory, is

$$\varphi_b = \varphi_m - E_A \tag{B1}$$

where φ_m is the work function of the metal, and E_A is the electron affinity of the semiconductor. In general, poor correlation is obtained between the barrier height predicted by Eq. (B1) and that measured experimentally.

In order to show this clearly, Figs. B1 through B4 were prepared for four semiconductors for which values of electron affinity were known and for which barrier height measurements have been taken for a number of metals. The values of work function used were the average values tabulated by Michaelson.[31] The spreads in work functions tabulated by Michaelson[31] are also shown by the horizontal lines. Electron affinity values were taken from Gobeli and Allen[32] for Si and GaAs, and from Kindig[33] for CdS. An electron affinity of 4.0 ev was arbitrarily assumed for GaP. The barrier height data were obtained from Cowley and Sze[17]* for Si and GaP, and from Spitzer and Mead[22] for CdS and GaAs. Data for CdS from Goodman[21] are also included in Fig. B2. In addition, data for Si are included in Fig. B1 from Crowell et al.[11]

---

*Cowley and Sze computed the Si barrier heights from data reported by Archer and Atalla.[34]

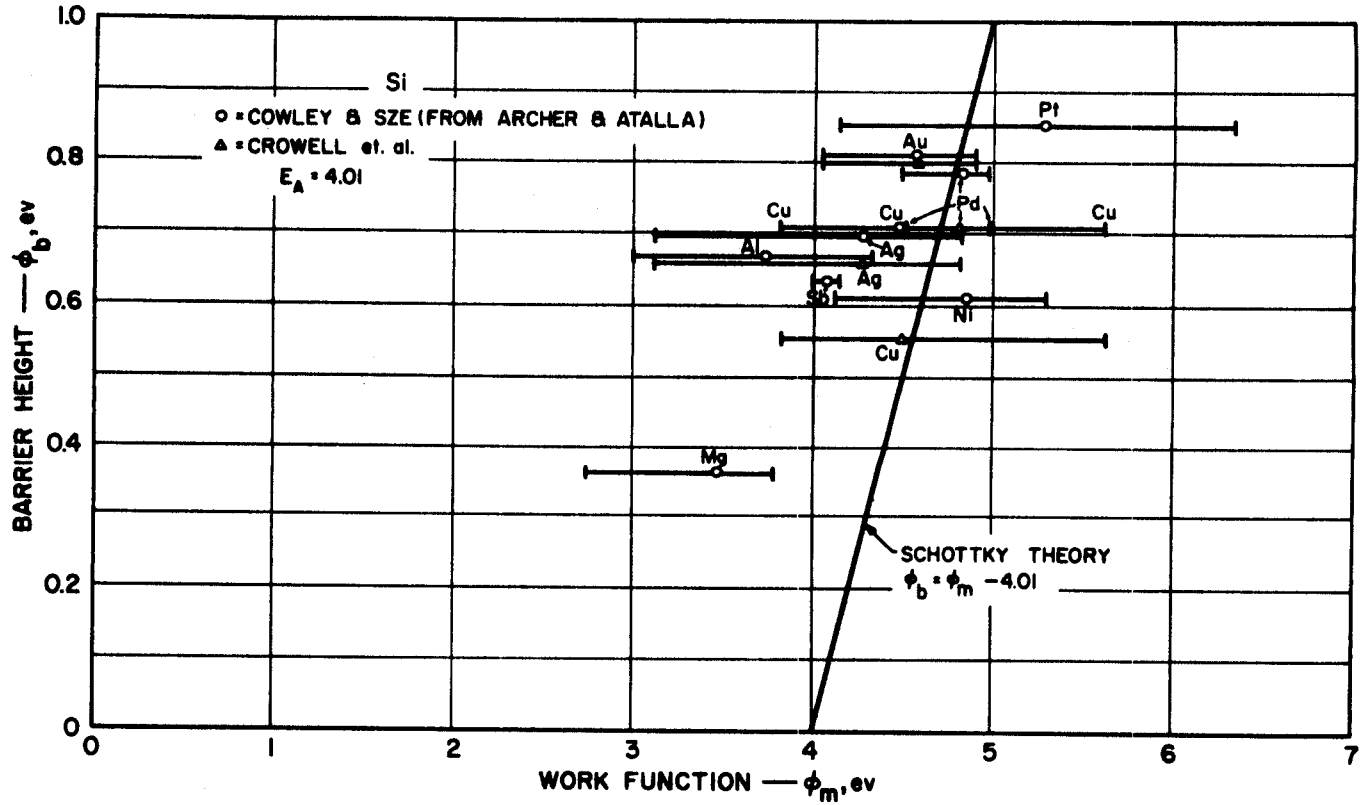

FIG. B-1 BARRIER HEIGHT VERSUS WORK FUNCTION FOR SEVERAL METALS ON SILICON.
The circles are the experimental barrier heights calculated by Cowley and Sze,[17] who used data reported by Archer and Atalla.[34] The work function values are from Michaelson.[31] The straight line is a plot of Eq. (B-1) using the electron affinity of 4.01 for Si as reported by Gobeli and Allen.[32]

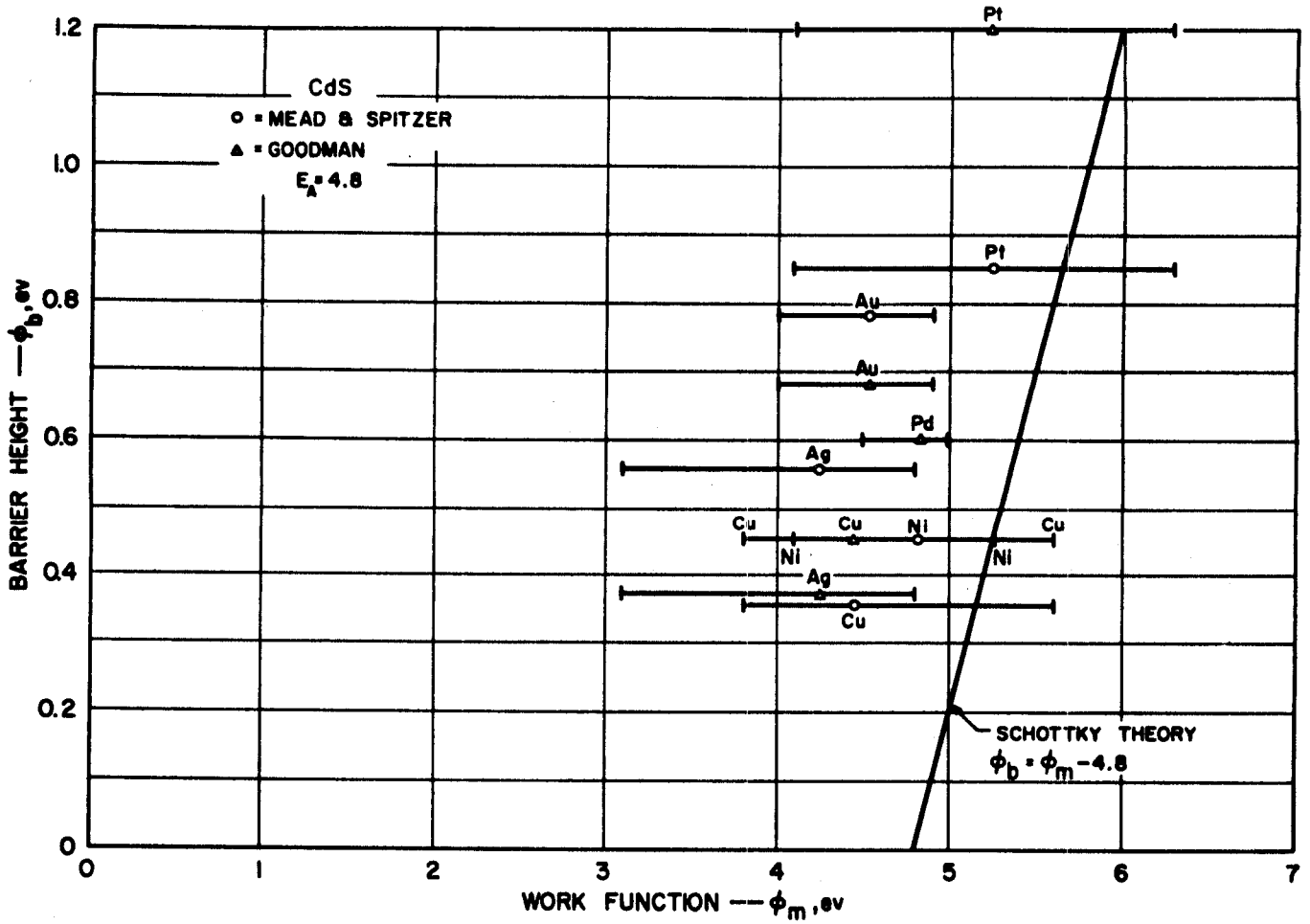

FIG. B-2 BARRIER HEIGHT VERSUS WORK FUNCTION FOR SEVERAL METALS ON CADMIUM SULFIDE.
The circles are the experimental barrier heights reported by Spitzer and Mead.[22] The work function values are from Michaelson.[31] The straight line is a plot of Eq. (B-1) using the electron affinity of 4.8 ev reported by Kindig.[33]

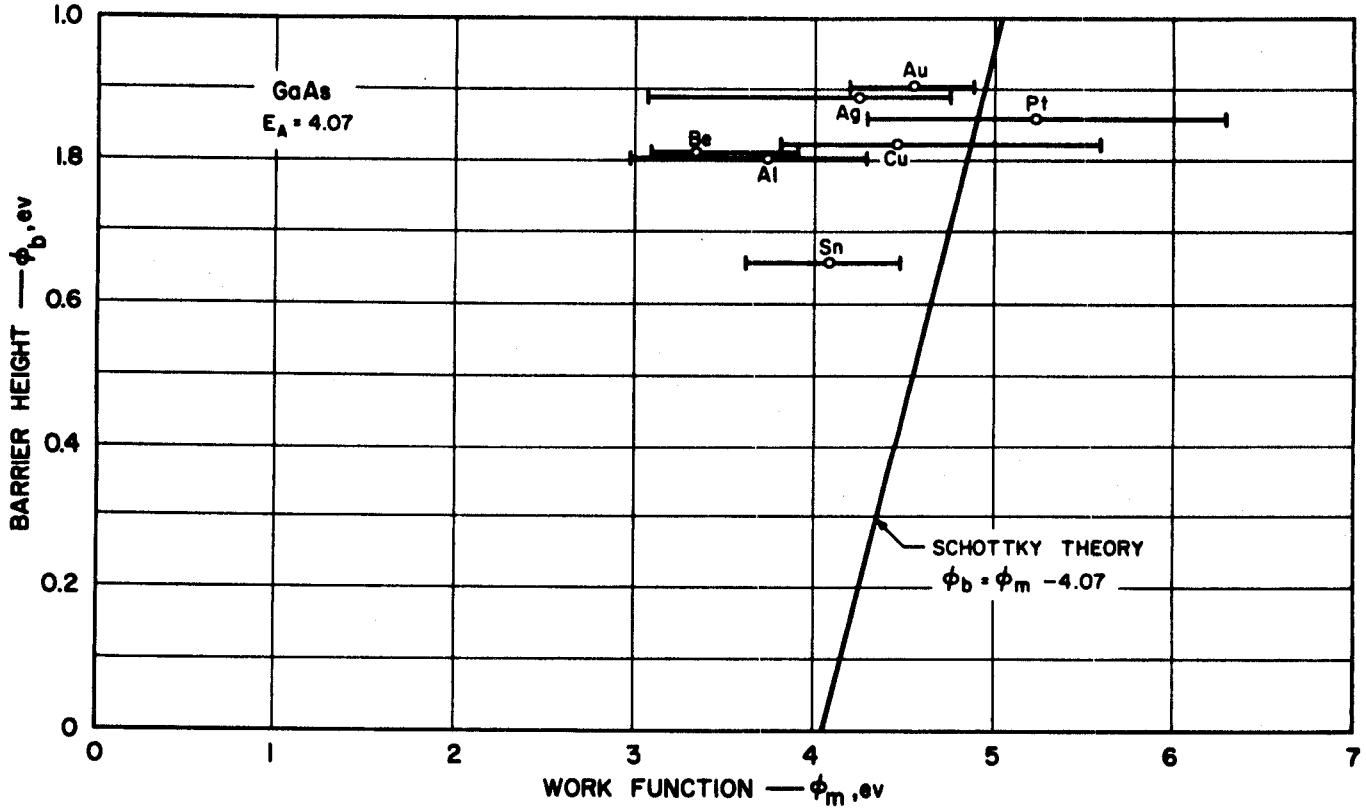

FIG. B-3 BARRIER HEIGHT VERSUS WORK FUNCTION FOR SEVERAL METALS ON GALLIUM ARSENIDE.
The circles are the experimental barrier heights reported by Spitzer and Mead.[22] The work function values are from Michaelson.[31] The straight line is a plot of Eq. (B-1) using the electron affinity of 4.07 ev reported by Gobeli and Allen.[32]

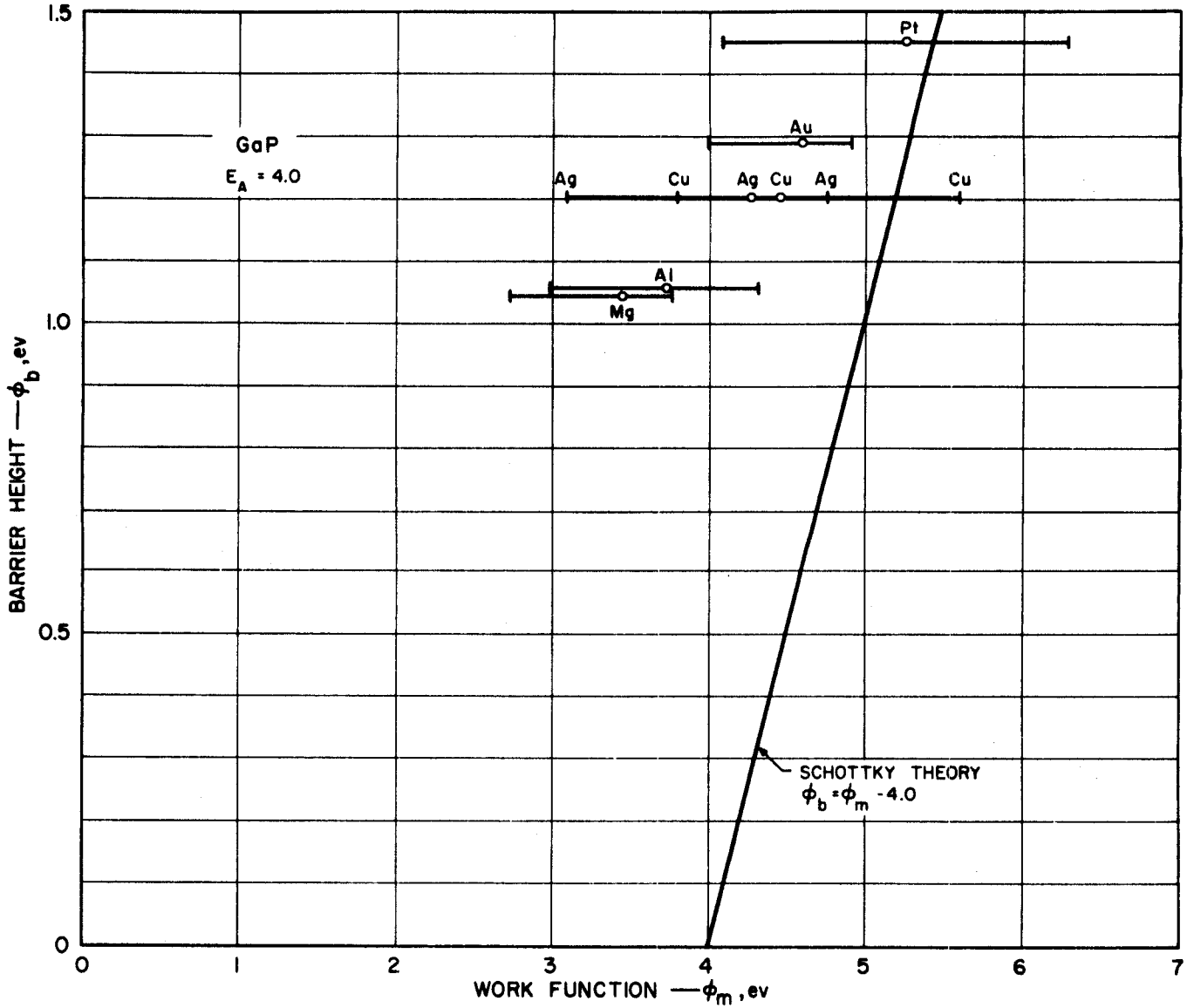

FIG. B-4 BARRIER HEIGHT VERSUS WORK FUNCTION FOR SEVERAL METALS ON GALLIUM PHOSPHIDE.
The circles are the experimental barrier heights reported by Cowley and Sze.[17] The work function values are from Michaelson.[31] The straight line is a plot of Eq. (B-1) using the electron affinity estimated by Cowley and Sze.[17]

In studying the lack of agreement between Schottky theory and experiment, the authors came to two related conclusions. First, it should be recognized that the magnitude of the difference between two numbers that are very nearly the same is very sensitive to the exact values of the two numbers. Thus, a very small percentage error in either φ_m or E_A in Eq. (B1) could produce a very large percentage error in the calculated value of φ_b. Second, the use of the mean values of work function tabulated by Michaelson[31] is, in general, not justified. For most metals there is a considerable spread in the values of work function reported by different workers, as noted in Figs. B1 through B4. This large spread is understandable because the work function of a metal is typically quite sensitive to surface contamination. In the case of thermionic emission, the surface may in some cases--for example, tungsten--be cleaned by the heating process; however, in the case of photoelectric emission or the contact potential method of measuring work function, the metal would have to be outgassed thoroughly in an ultra-high vacuum system before the work function measurement could take on any real significance. Or, alternatively, measurements could be made on freshly evaporated films in an ultra-high vacuum.

These precautions were not always observed by the various workers, and many of the values are therefore unreliable. Reliable measurements have been made for some metals in recent years, as will be discussed later. However, it has come to be recognized that the work function of an evaporated metal film may vary several tenths of a volt from the bulk value, and that annealing of such evaporated films can cause large changes in work function. In addition, the substrate can exert a considerable influence on the structure of the condensing film and consequently the work function.

This paper will first consider the following question: Can Eq. (B1) be made to agree with experiment through the use of the correct* work function for each metal? Assuming the answer to this question is in the

*"Correct" here means the work function of a metal film evaporated in an ultra-high vacuum onto a cold substrate identical to that used for the metal-semiconductor barriers of Figs. B1 through B4.

affirmative, a second question then arises: Can the correct values of work function be found from the experimental barrier height data? A third question concerns the values of electron affinity for the semiconductors--i.e., Can correlation be found between the independently measured electron affinity values and the values required to make Eq. (B1) fit experiment? It is the purpose of this paper to attempt an answer to these questions. Conclusions concerning the validity of Eq. (B1) can then be drawn. It will be shown that electron affinity values can be made to fit by modifying Eq. (B1) to include the effects of surface states.

2. Calculations

As a first step in attempting to answer the preceding questions, Table BI was prepared.

The third column in Table BI consists of the mean values of work function for each metal as tabulated by Michaelson.[31]* The fourth column consists of the experimental values of barrier height. The fifth column consists of the electron affinity values required to fit Eq. (B1). The electron affinity values were then averaged for each semiconductor, as listed in the sixth column of Table BI. Equation (B1) was then solved for φ_m for each metal on each semiconductor, using the average values of electron affinity. The seventh column of Table BI shows the results of these calculations, the values being referred to as the adjusted work function values.

We can now compare the adjusted values of φ_b for the same metal on different semiconductors and thereby answer the first question raised. Table BII lists these adjusted φ_b values, and it can be seen that reasonably good agreement is indeed obtained between the values of adjusted φ_b for the same metal on different semiconductors. The worst deviations occur for CdS, the values being consistently high for this semiconductor. The average value of φ_b for each metal was then found; these results are shown in Table BIII.

*The mean values of more recent tables could have been used; but, as will be shown, the final results and conclusions would not be significantly altered.

Table B-I

ELECTRON AFFINITY AND ADJUSTED WORK FUNCTION VALUES ACCORDING TO SCHOTTKY THEORY

Semiconductor (n-type)	Metal	Mean Work Function (Michaelson[31]) (ev)	Experimental Barrier Height (ev)	E_A Required to Fit Eq. (B-1) (ev)	Average E_A for each Semiconductor (ev)	Adjusted Work Function (ev)
Si (Cowley and Sze[17])	Mg	3.46	0.36	3.10	3.72	4.08
	Cu	4.47	0.71	3.76		4.43
	Sb	4.08	0.63	3.45		4.35
	Ni	4.84	0.61	4.23		4.33
	Ag	4.28	0.69	3.59		4.41
	Al	3.74	0.67	3.07		4.39
	Pd	4.82	0.78	4.04		4.50
	Au	4.58	0.81	3.77		4.53
	Pt	5.29	0.85	4.44		4.57
Si (Crowell et al.[11])	Ag	4.28	0.66	3.62	3.86	4.52
	Cu	4.47	0.55	3.92		4.41
	Au	4.58	0.80	3.78		4.66
	Pd	4.82	0.71	4.11		4.57
CdS (Spitzer and Mead[22])	Au	4.58	0.78	3.80	4.09	4.87
	Ag	4.28	0.56	3.72		4.65
	Cu	4.47	0.36	4.11		4.45
	Ni	4.84	0.45	4.39		4.54
	Pt	5.29	0.85	4.44		4.94
CdS (Goodman[21])	Au	4.58	0.68	3.90	4.03	4.71
	Pd	4.82	0.60	4.22		4.63
	Cu	4.47	0.45	4.02		4.48
	Ag	4.28	0.37	3.91		4.40
	Pt	5.29	1.20	4.09		5.23
GaAs (Spitzer and Mead[22])	Au	4.58	0.90	3.68	3.45	4.35
	Al	3.74	0.80	2.94		4.25
	Ag	4.28	0.88	3.40		4.33
	Cu	4.47	0.82	3.65		4.27
	Pt	5.29	0.86	4.43		4.31
	Be	3.37	0.81	2.56		4.26
	Sn	4.11	0.65	3.46		4.10
GaP (Cowley and Sze[17])	Mg	3.46	1.04	2.42	3.10	4.14
	Al	3.74	1.05	2.69		4.15
	Ag	4.28	1.20	3.08		4.30
	Cu	4.47	1.20	3.27		4.30
	Au	4.58	1.28	3.30		4.38
	Pt	5.29	1.45	3.84		4.55

Table B-II

COMPARISON OF ADJUSTED WORK FUNCTIONS FROM TABLE B-I

Semiconductor → Metal	Si (Cowley and Sze)	Si (Crowell et al.)	CdS (Spitzer and Mead)	CdS (Goodman)	GaAs	GaP
Mg	4.08					4.14
Cu	4.43	4.41	4.45	4.48	4.27	4.30
Sb	4.35					
Ni	4.33		4.54			
Ag	4.41	4.52	4.65	4.40	4.33	4.30
Al	4.39				4.25	4.15
Pd	4.50	4.57		4.63		
Au	4.53	4.66	4.87	4.71	4.35	4.38
Pt	4.57		4.94	5.23	4.31	4.55
Be					4.26	
Sn					4.10	

Table B-III

AVERAGE OF ADJUSTED WORK FUNCTIONS FROM TABLE B-II

Metal	Average Adjusted Work Functions (ev)
Mg	4.11
Cu	4.39
Sb	4.35
Ni	4.44
Ag	4.44
Al	4.26
Pd	4.57
Au	4.58
Pt	4.72
Be	4.26
Sn	4.10

The foregoing procedure is tantamount to assuming that although the mean work function values tabulated by Michaelson[31] are unreliable, the average value of work function for all the metals is probably close to the average value of the correct work functions. The procedure then assumes that the electron affinities of the semiconductors used in Table BI are unknown, and the first step is to find these electron affinities. Assuming Eq. (B1) is valid and the Michaelson[31] average values apply, an average of the electron affinity values of the fifth column should be close to the correct electron affinity for each semiconductor. These averages are shown in the sixth column of Table BI. The next step is to find the adjusted work functions that fit Eq. (B1). These are shown in the seventh column of Table BI and listed in Table BII. The next assumption is that the average values of work function of Table BII are close to the correct work functions. These averages are listed in Table BIII.

An iterative procedure is then employed, as shown in Table BIV. This table is like Table BI, except that the average adjusted work functions of Table BIII were used instead of the mean work function values of Michaelson.[31] It can be seen that the various values of electron affinity in the fourth column of Table BIV are much more consistent for each semiconductor than was the case for Table BI. The average value of electron affinity for each semiconductor is then found, as shown in the fifth column of Table BIV. New readjusted work functions for each metal on each semiconductor are then found, as shown in the sixth column of Table BIV and as listed in Table BV. It can be seen that the values for CdS are no longer consistently high, as they were in Table BII. The average value of work function for each metal listed in Table BV was then found, as shown in the fourth column of Table BVI. These values will subsequently be referred to as the derived values of work function.

The foregoing procedure could be iterated, but the close agreement between the average E_A values in Tables BI and BIV and between the φ_m values of Tables BIII and BVI indicate that only insignificant changes would occur.

Figures B5 through B8 were then prepared, using the average values

Table B-IV

ADJUSTED ELECTRON AFFINITY AND READJUSTED WORK FUNCTION VALUES ACCORDING TO SCHOTTKY THEORY

Semiconductor	Metal	Average Adjusted Work Function (ev)	E_A Required to Fit Eq. (B-1) (ev)	Average E_A for each Semiconductor (ev)	Readjusted Work Function (ev)
Si (Cowley and Sze[17])	Mg	4.11	3.75	3.75	4.11
	Cu	4.39	3.68		4.46
	Sb	4.35	3.72		4.38
	Ni	4.44	3.83		4.36
	Ag	4.44	3.75		4.44
	Al	4.26	3.59		4.42
	Pd	4.57	3.79		4.53
	Au	4.58	3.77		4.56
	Pt	4.72	3.87		4.60
Si (Crowell et al.[11])	Ag	4.44	3.78	3.81	4.47
	Cu	4.39	3.84		4.36
	Au	4.58	3.78		4.61
	Pd	4.57	3.86		4.52
CdS (Spitzer and Mead[22])	Au	4.58	3.80	3.91	4.69
	Ag	4.44	3.88		4.47
	Cu	4.39	4.03		4.27
	Ni	4.44	3.99		4.36
	Pt	4.72	3.87		4.76
CdS (Goodman[21])	Au	4.58	3.90	3.88	4.56
	Pd	4.57	3.97		4.48
	Cu	4.39	3.94		4.33
	Ag	4.44	4.07		4.25
	Pt	4.72	3.52		5.08
GaAs (Spitzer and Mead[22])	Au	4.58	3.68	3.58	4.48
	Al	4.26	3.46		4.38
	Ag	4.44	3.56		4.46
	Cu	4.39	3.57		4.40
	Pt	4.72	3.86		4.44
	Be	4.26	3.45		4.39
	Sn	4.10	3.45		4.23
GaP (Cowley and Sze[17])	Mg	4.11	3.07	3.21	4.25
	Al	4.26	3.21		4.26
	Ag	4.44	3.24		4.41
	Cu	4.39	3.19		4.41
	Au	4.58	3.30		4.49
	Pt	4.72	3.27		4.66

Table B-V

COMPARISON OF READJUSTED WORK FUNCTIONS FROM TABLE B-IV

Semiconductor → Metal	Si (Cowley and Sze)	Si (Crowell et al.)	CdS (Spitzer and Mead)	CdS (Goodman)	GaAs	GaP
Mg	4.11					4.25
Cu	4.46	4.36	4.27	4.33	4.40	4.41
Sb	4.38					
Ni	4.36		4.36			
Ag	4.44	4.47	4.47	4.25	4.46	4.41
Al	4.42				4.38	4.26
Pd	4.53	4.52		4.48		
Au	4.56	4.61	4.69	4.56	4.48	4.49
Pt	4.60		4.76	5.08	4.44	4.66
Be					4.39	
Sn					4.23	

Table B-VI

COMPARISON OF WORK FUNCTION VALUES

Metal	Michaelson's Mean φ_m (ev)	Recent Measurements of φ_m (ev)	Derived Values of φ_m (ev)
Mg	3.46	(3.68)*	4.18
Cu	4.47	4.52 ± 0.04,[40] 4.39,[39] 4.39[35]	4.37
Sb	4.08	(4.25)*	4.38
Ni	4.84	4.74 ± 0.04,[40] 4.59,[35] 5.0,[39] 5.14[42]	4.36
Ag	4.28	4.31 ± 0.03,[40] 4.38,[39] 4.23[35]	4.42
Al	3.74	4.20 ± 0.05[40]	4.35
Pd	4.82	4.95 ± 0.05,[40] 4.95[35]	4.51
Au	4.58	4.70 ± 0.03,[40] 4.83 ± 0.02,[41] 4.8[39]	4.56
Pt	5.29	5.48[35]	4.71
Be	3.37	(3.92)*	4.39
Sn	4.11	4.33[35]	4.23

*See explanation in text.

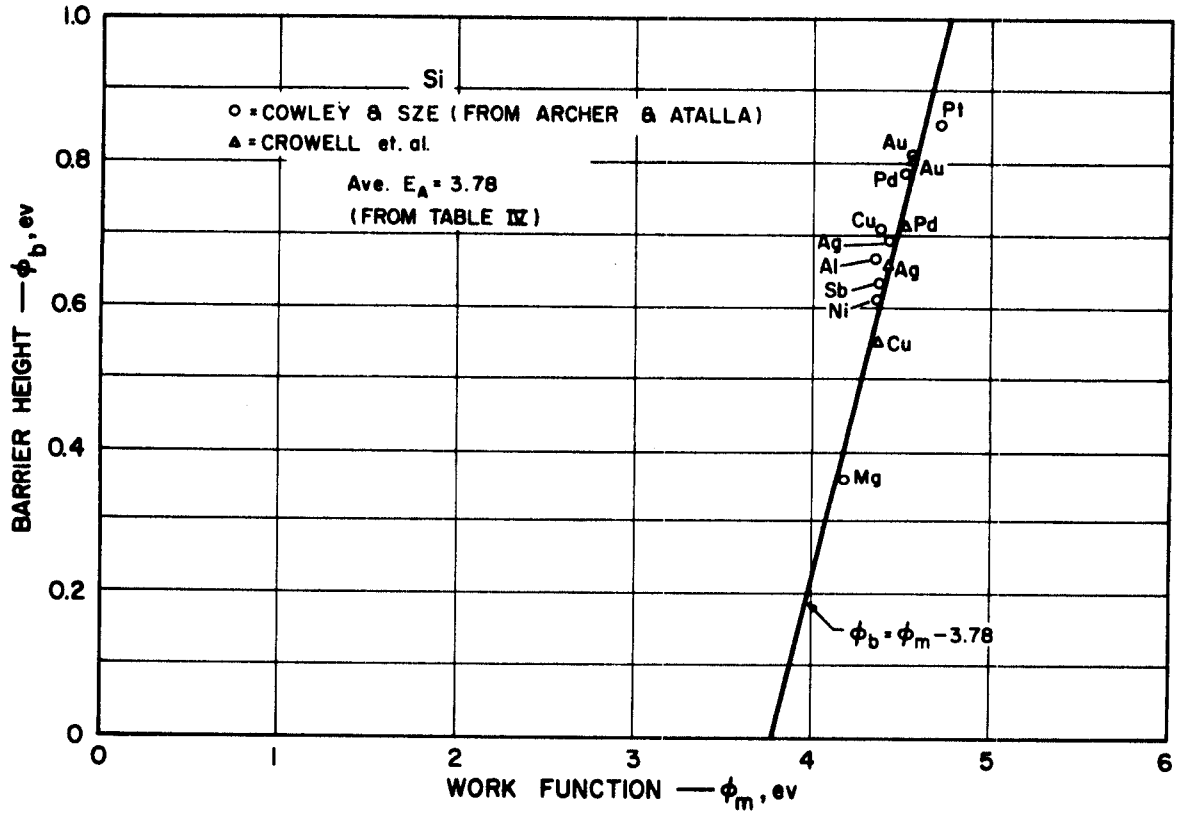

FIG. B-5 BARRIER HEIGHT VERSUS WORK FUNCTION FOR SEVERAL METALS ON SILICON.
The circles are the experimental barrier heights calculated by Cowley and Sze[17] using data reported by Archer and Atalla.[34] The work function values are those determined by means explained in the text. The straight line is a plot of Eq. (B-1) using the electron affinity of 3.69 ev determined by means explained in the text.

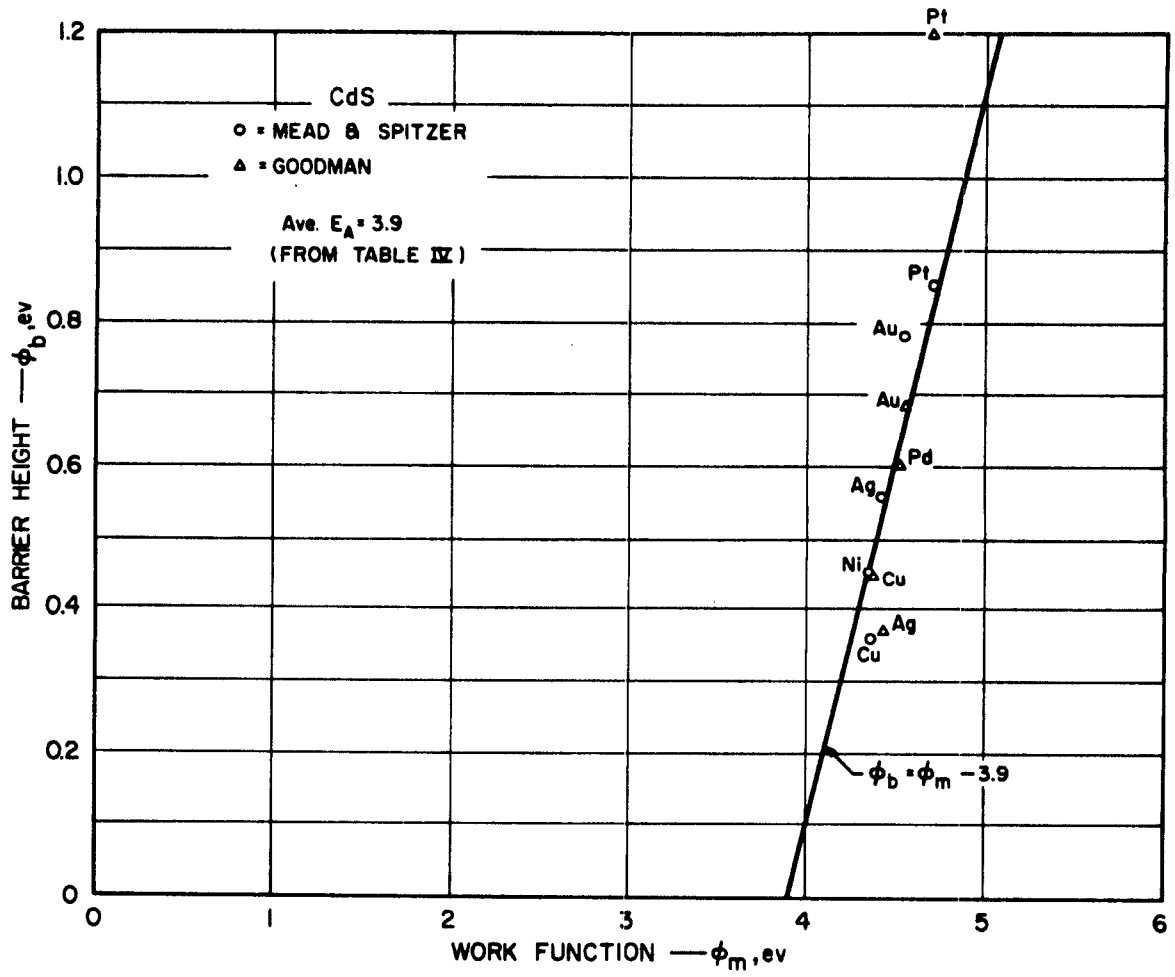

FIG. B-6 BARRIER HEIGHT VERSUS WORK FUNCTION FOR SEVERAL METALS ON CADMIUM SULFIDE.
The circles are the experimental barrier heights reported by Spitzer and Mead.[22] The work function values are those determined by means explained in the text. The straight line is a plot of Eq. (B-1) using the electron affinity of 3.87 ev determined by means explained in the text.

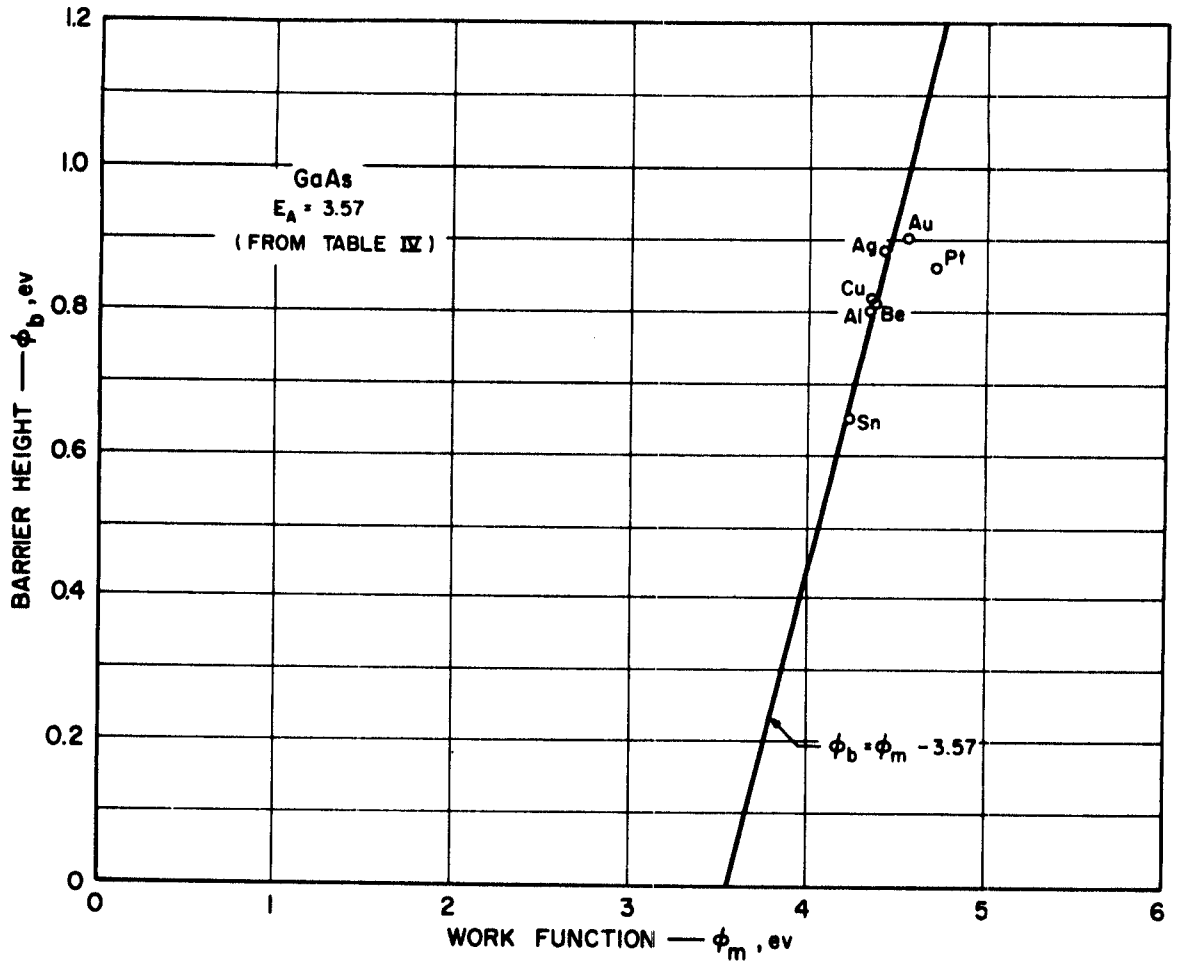

FIG. B-7 BARRIER HEIGHT VERSUS WORK FUNCTION FOR SEVERAL METALS ON GALLIUM ARSENIDE. The circles are the experimental barrier heights reported by Spitzer and Mead.[22] The work function values are those determined by means explained in the text. The straight line is a plot of Eq. (B-1) using the electron affinity of 3.56 ev determined by means explained in the text.

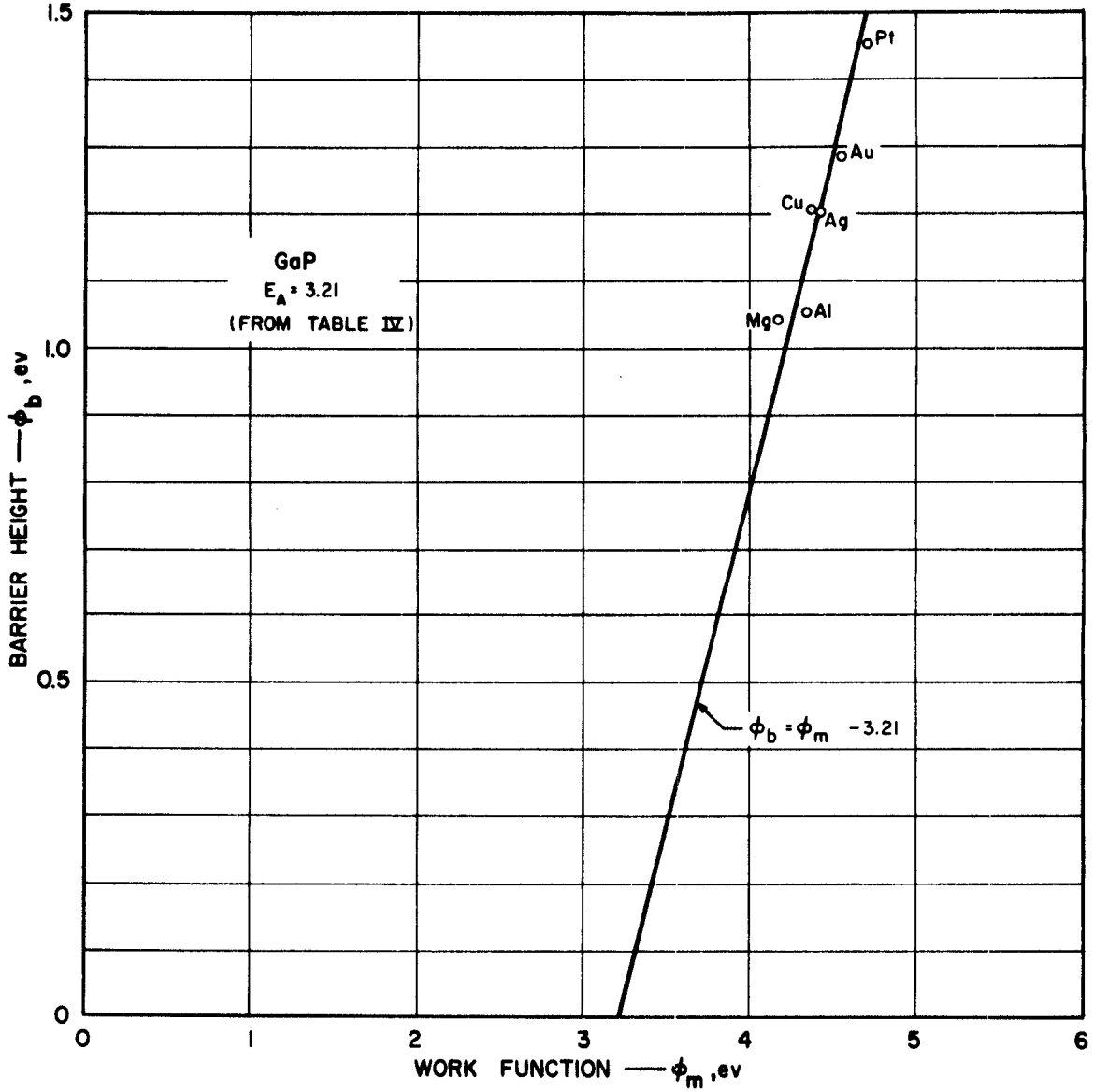

FIG. B-8 BARRIER HEIGHT VERSUS WORK FUNCTION FOR SEVERAL METALS ON GALLIUM PHOSPHIDE. The circles are the experimental values reported by Cowley and Sze.[17] The work function values are those derived by means explained in the text. The straight line is a plot of Eq. (B-1) using the electron affinity of 3.17 ev determined by means explained in the text.

of E_A from Table BIV and the derived values of φ_m of Table BVI. The agreement between theory and experiment using the derived values of E_A is seen to be quite satisfactory.

We are now in a position to judge the validity of Eq. (B1). We shall proceed to do this in two ways; first, we will compare some of the derived work function values with values measured recently under meaningful conditions. Second, we will compare the derived electron affinity values with those measured by photoelectric experiments.

3. Comparison of Work Functions

The values of φ_m in the third column of Table BVI are recent measurements made on thin films evaporated onto glass substrates. In all cases the films were evaporated and measured in vacuums of 10^{-8} torr, or better. The thinnest films--i.e., $\sim$ 100 Å--were used by Suhrmann and Wedler.[35] They report no dependence of φ_m on thickness for films greater than 50 Å. This is confirmed by Bryla and Feldman[36] for films of Au, Ag, and Pt.

There is a dependence of φ_m on the structure of the film as reported by Suhrmann and Wedler[35] and others.[37,38] This dependence is related in turn to the type of substrate, the method of deposition, and particularly to any heat treatment during and following deposition. The values quoted from Suhrmann and Wedler[35] and Culver et al.[39] are for films deposited on substrates at 77°K or 90°K. The other values are for films deposited on substrates at room temperature. All the values of φ_m were measured without subsequent heating of the films. It is interesting to note that increases of the order of 0.5 ev in the values of φ_m are reported by Suhrmann and Wedler[35] when the films are heated to 100°C or 200°C.

The measurements were made by a variety of techniques. Reviève[40] measured the contact potential differences with respect to W , for which he used a φ_m value of 4.565 ± 0.025 ev. Culver et al.[39] used a retarding potential technique. P. A. Anderson[41] measured the contact potential difference between Au and Ba, using a value of 2.52 ev for Ba. Suhrmann and Wedler[35] and Anderson and Klemperer[42] made photoelectric measurements.

No recent values could be located for Mg, Sb, or Be films that were prepared and measured by methods comparable to those described. Additional values for the other metals listed were rejected on a similar basis. A later tabulation by Michaelson[43] selects preferred values for Mg and Be from the values used in his original tabulation. They are 3.68 ev and 3.92 ev, respectively. In the case of Sb no preferred value is indicated, but an additional value of 4.60 ev is included, which would bring the mean value for Sb up to 4.25 ev.

A review of Michaelson's[43] tabulated values for Zn, Cd, Sr, Ca, Ba, Mg, Be, and Al indicates a steady increase in the measured values of φ_m over the years, from the early measurements in the 1920's to the later measurements in the 1950's. For many of these metals it is known that the work function of the metal oxide is lower than that of the corresponding metal. It seems reasonable, then, to attribute this increase in work function over the years to improved vacuum technology. Partial oxidation of Sr, Ca, or Ba during preparation and testing would certainly reduce the value of φ_m .[5] In the case of Mg, Stevenson and Hensley[44] report work function values for the oxide ranging from 2.31 ev to 3.70 ev. For Al, Chapman[45] gives a value in the vicinity of 3.9 ev for the oxide. Since these values are less than the respective values of φ_m for the metal, partial oxidation due to inadequate vacuums would help to explain the large change in work function values. Since Be is also a Group II element, a similar argument should apply to the measurement of its work function.

The values of φ_m derived by the reiterative process for Mg, Al, and Be are in better agreement with the more recently measured values listed in the third column of Table BVI than with the average values of Michaelson's original tabulation[31] listed in the second column. Barrier height data for Mg and Be are limited; but if the Schottky model is correct, the derived values of φ_m obtained from the barrier height measurements may be indicative of the values that will be measured ultimately by other techniques.

Another effect should be considered with metals like Pd and Pt.

Prior to the advent of electron-beam heating for evaporation, it was difficult to prepare pure films of these metals. With prolonged evaporations from resistance-heated sources, traces of impurities with lower work functions could have been deposited along with the metal in question.

Considering the difficulties encountered in making meaningful measurements of φ_m, and the many factors involved in preparing thin films of metals, the final values of φ_m derived in this paper from barrier height measurements should be verified experimentally. The work functions of the metals used to form the barriers should be measured on the same structure on which the barrier height is measured. In this way the need for correlating substrate effects and deposition techniques from separate measurements of φ_m will be eliminated. Even with this procedure there may be some variation between the effective work function at the metal-semiconductor interface and that measured at the metal-vacuum interface. In this connection it would be desirable to use the thinnest continuous film possible.

4. Comparison of Electron Affinities

The average electron affinity values of Table BIV may now be compared with the available experimental values for this quantity. Gobeli and Allen[32] report a value of 4.01 ev for the electron affinity of Si, based on a rather involved interpretation of their photoelectric emission data from vacuum-cleaned Si surfaces.[46] They used "atomically flat" surfaces for their experiments, obtained by a special cleaving technique. This refinement was an important consideration in the interpretation of their data; for as has been pointed out by Kane[47] in a theoretical treatment of photo-emission processes from semiconductors, the condition of the semiconductor surface has an important effect on the scattering of photo-excited electrons as they leave the semiconductor, and hence affects the yield-vs.-photon energy relationship near threshold. Recent work by Van Laar and Scheer[48] on Si surfaces prepared by fracturing Si in high vacuum has disclosed a dependence of photoelectric yield on photon energy; this presumably can be ascribed to the condition of the Si surface, since it is observed in general that fractured surfaces are highly imperfect compared to those prepared by the method of Allen and Gobeli.[49] The electron

affinity inferred from the data of Van Laar and Scheer is about 4.3 ev, according to their assumption that the photoelectric yield "tail" in their experiments is due to emission from surface states.[50] This assumption has been criticized by Gobeli and Allen,[32] and it seems equally reasonable on the basis of Kane's treatment[47] to ascribe the "tail" emission observed by Van Laar and Scheer to transitions from volume states in the valence band near the surface with the rough surface acting as a momentum absorber. This interpretation results in an electron affinity of 3.75 ev for the broken or "imperfect" Si surface. This value agrees well with the value derived in this work (Table BIV). It is certainly reasonable to compare the surfaces used by Archer and Atalla[34] for the preparation of the metal-Si contacts to the surfaces used by Van Laar and Scheer, rather than to those used by Gobeli and Allen, since Archer and Atalla used no special precautions to insure "atomically flat" surfaces as did Gobeli and Allen. However, the question of the correct interpretation (i.e., surface states-vs.-valence band) of Van Laar and Scheer's photo-emission data is still open at this time.

The electron affinity of vacuum-cleaved GaAs is reported by Gobeli and Allen[32] to be 4.07 ev. This is at variance with the value of 3.58 ev inferred in this work (Table BIV), but it will be pointed out in the next section that a plausible explanation for this discrepancy can be formulated in terms of surface electronic states below the Fermi level at the GaAs surface. Gobeli and Allen[32] report that GaAs crystals are more easily cleaved than Si, and suggest that cleavages performed using ordinary techniques (e.g., the technique used by Spitzer and Mead[22]) are likely to produce atomically flat surfaces. It is therefore reasonable to assume that the surfaces used by Gobeli and Allen and by Spitzer and Mead were nearly identical, and that the electron affinity inferred by Gobeli and Allen is appropriate also to the metal-GaAs junctions. The electron affinity of CdS obtained in this work is about 3.9 ev, using either the data of Spitzer and Mead[22] (cleaved surfaces) or of Goodman[21] (chemically cleaned substrates). Kindig[33] has reported a value of 4.8 ev for the electron affinity of CdS crystals cleaved in ultra-high vacuum, and has estimated the electron affinity for samples cleaved in air at

$\sim$ 3.8 ev. There is apparently good correspondence between the value obtained here from Goodman's data and the estimate of Kindig, since the surfaces in both experiments are expected to be contaminated by oxide and/or adsorbed air molecules. A possible explanation for the discrepancy in the vacuum-cleaved cases is offered in the next section.

No conclusions regarding the electron affinity for GaP can be drawn at this time, since the only published "value" currently available in the literature is the estimate of Cowley and Sze.[17]

5. Surface States

It is well established, both theoretically[51] and experimentally,[52] that localized electronic states occur in the forbidden gap at a free semiconductor surface. It is expected that there will be roughly two surface states per surface atom, and that these states will be more or less uniformly distributed in energy in the forbidden gap.[51] Surface states have been invoked by Bardeen[53] to explain both the relative constancy of semiconductor work function with large changes in bulk Fermi level, and the apparent lack of strong dependence of barrier height in metal-semiconductor diodes on metal work function. Recent investigations of metal-semiconductor systems seem to confirm the presence of surface states in these junctions.[17,22,34] Heine[54] has recently challenged the customary view of surface states in metal-semiconductor junctions, in which the states are assumed to have the same origin as the so-called Shockley states at the free surface. He objects to this view mainly because many of the most recent experiments on metal-semiconductor systems have been performed using evaporated metal contacts on cleaved semiconductor surfaces. There is every reason to believe that this technique produces metal-semiconductor contacts that are intimate on an atomic scale, and, strictly speaking, no "surface states" should exist in such a junction. Heine proceeds, however, to show that the "tails" of the metallic electron wave-functions which exist in the semiconductor (or, in some cases, vice-versa) produce electronic states in the forbidden gap near the semiconductor surface which, for practical purposes, have the same effect on the variation of the potential barrier

height with work function as do true "surface states." It is the purpose of this section to show that, whatever the mechanism for the existence of localized electronic levels at the semiconductor surface may be, it is possible to invoke these levels to explain the discrepancies in electron affinity noted in the last section.

The rough calculations of Heine[54] for Si indicate that a distribution (in energy) of electronic states, that is more dense near the edges of the band gap than in the center, exists in the semiconductor forbidden gap near the semiconductor-metal interface. His model predicts the highest density of states near the valence band. His estimate of the density of states averaged over the mean band gap of Si [$\sim$ 4.5 ev at the (111) plane] is 3.5×10^{14} states/ev/cm^2. This could mean that densities near the center of the optical band gap are low, perhaps 10^{12}/ev/cm^2, while densities near the band edges are higher, approaching 10^{13}/ev/cm^2 or higher. Adapting this picture of the density of surface states in the forbidden gap, we can conjecture that the filling of surface states up to some level φ_o near the valence band produces a neutral surface (half of the available states must fill up for neutrality, assuming two states per lattice site).[17]

If we denote the density of surface states at energy F by $N_{ss}(E)$ per cm^2 per ev, then the net charge in surface states, denoted by Q_{ss}, is given by

$$Q_{ss} = - e \int_{\varphi_o}^{F} N_{ss}(E)\, dE \qquad \text{(B2)}$$

in the $0^\circ K$ approximation to the Fermi function. If we assume that N_{ss} at the Fermi level is small, then most of the contribution to Q_{ss} is due to states below the Fermi level, and Q_{ss} is approximately independent of the position of E_F in the forbidden gap at the surface. In Appendix C the barrier height of a metal-semiconductor contact for this case is derived approximately as

$$\varphi_b \simeq (\varphi_m - E_A - \Delta \varphi_n) + V_3 \qquad \text{(B3)}$$

where φ_m is the metal work function, E_A the semiconductor electron affinity, and $\Delta\varphi_n$ the image force lowering. The V_3 term arises from the presence of surface states, as derived in Appendix C. The first three terms on the right side of this equation are equal to the barrier height for a Schottky barrier under the usual assumptions of no surface states at the junction. The added term V_3 arises from the surface states at the interface, and is a constant independent of Fermi level position under the assumption that significant contributions to Q_{ss} arise from high $N_{ss}(E)$ below the Fermi level.

The appearance of the V_3 term in Eq. (B3) can explain the low values of electron affinity for Si and GaAs calculated on the basis of Eq. (B1). The number of surface states below the Fermi level necessary to account for these discrepancies is on the order of 10^{13} states/cm^2, assuming $\delta = 10$ Å, $\epsilon_i = \epsilon_o$.

A surface state distribution having the form described above might also explain the deviation of Au and Pt points from the GaAs line (Fig. B7): As the barrier height tends to increase, the Fermi level finally enters the region of high $N_{ss}(E)$ near the valence band edge, and the slope of φ_b vs. φ_m is reduced sharply. The extreme case treated in Appendix C (delta-function of surface-states) results in a horizontal φ_b vs. φ_m relation.

6. Discussion

The interpretation, in terms of Eq. (B3), of the available barrier height data for metal-semiconductor junctions is an alternative to that given by Cowley and Sze.[17] We initially assumed, contrary to Cowley and Sze, that Schottky theory is valid, i.e., the barrier height varies in direct proportion to changes in the metallic work function. The investigation of the barrier height-vs.work-function data for four semiconductors reveals that a self-consistent set of metallic work functions may be derived from the barrier height data, assuming the validity of the Schottky theory. The values for metal work functions obtained in this way are not unreasonable in view of the wide spread in published work-function values for most metals.[31] In fact, the work-function values

obtained here are generally in agreement with recently measured values obtained for thin films under conditions of ultra-high vacuum.

Cowley and Sze obtained a least-squares straight line fit to the same barrier height-vs.-work-function data used in the present paper. With the exception of the CdS data of Goodman,[21] the resulting straight lines had slopes of much less than unity, indicating that Schottky theory is apparently not applicable in these cases. However, it should be recognized that the slopes of the lines obtained by this procedure are extremely sensitive to the values chosen for the work functions of the metals. Referring to the GaP data in Fig. B4, for example, one can see that taking the Pt work function to be 4.6 ev[6] has a marked effect on the slope of the fitted line; if in addition φ_m (Mg) is taken to be about 4.0 ev, and φ_m (Al) is taken as Rivière's[40] recently measured value of 4.2 ev, a line whose slope is essentially unity can be fitted to the data. A similar argument holds for Si and GaAs.

7. Conclusions

On the basis of the thoughts presented in this paper, the authors have drawn the following conclusions:

(1) The presently available barrier height-vs.-work-function data for Si, GaP, GaAs, and CdS are probably inadequate for the purpose of deriving or verifying a quantitative theory for the barrier height of metal contacts to these semiconductors. A larger number of experimental points is needed to clearly establish the form of the φ_b-vs.-φ_m relationship.

(2) Measurements of metallic work function reported in the literature have been performed under conditions which in general do not duplicate the structure of a metal film on a single-crystal semiconductor substrate. Since it is well-known that the metallic work function is sensitive not only to the condition of the metal surface, but also to the crystal structure of the bulk metal, it would seem that attempts at correlation of barrier height with metallic work function are meaningful only if the work function and barrier height measurements are performed using films of a given metal whose bulk and surface properties are identical.

(3) In the interest of eliminating as many experimental "variables" as possible, it is important that in measurements of barrier height and electron affinity, the same crystal face of a given semiconductor be used. Comparison of, for example, electron affinities obtained by photothreshold and barrier height measurements, each on a different semiconductor crystal face, would be meaningless.* Recent experiments on silicon vacuum-cleaved surfaces[55] show that heat treatment (annealing) of the crystals has a marked effect on both the electron affinity and the distribution of surface states. This work emphasizes the importance of insuring uniform surface treatment of semiconductors that are to be used in experiments attempting to correlate surface properties with barrier height.

It is hoped that the work presented herein will stimulate further experimental effort along the lines indicated in the conclusions above. An experiment that could shed much light on the question of the dependence of φ_b on φ_m is the evaporation of barium contacts onto the various semiconductors listed in the text of this paper. Barium has a work function that is fairly well established at ~ 2.5 ev, and would provide a point in the φ_b-vs.-φ_m data which is well beyond the range of the present data. Cesium would also be a candidate for an experiment of this type, but the experimental difficulties in evaporating a pure layer of cesium onto a localized region of semiconductor would be greater.

*D. Kahng, for example, [Bell Syst. Tech. J., 43, p. 215 (1964)][56] observes that for GaAs-metal surface diodes, the barrier height φ_b is strongly dependent on the crystallographic orientation of the semiconductor surface used to fabricate the diodes.

APPENDIX C

POTENTIAL BARRIER IN METAL-SEMICONDUCTOR SYSTEM WITH DISCRETE SURFACE STATE LEVEL

APPENDIX C

POTENTIAL BARRIER IN METAL-SEMICONDUCTOR SYSTEM WITH DISCRETE SURFACE STATE LEVEL

1. Free Semiconductor Surface

The energy band diagram of an n-type semiconductor surface is shown in Fig. C-1. The surface-state neutrality level φ_o[17] is assumed to lie somewhere below the discrete surface state level shown on this diagram. Filling up this level corresponds, therefore, to charging the surface negatively. In equilibrium for the free surface, the surface states fill up and the semiconductor bands must bend up to uncover a sufficient number of donor ions to provide overall charge neutrality, i.e.,

$$Q_{ss} + Q_{sc} = 0 \qquad \text{(C-1)}$$

where Q_{ss} is the charge in surface states, and Q_{sc} is the semiconductor space charge. The surface states charge Q_{ss} is given by

$$Q_{ss} = - e N_{ss} \qquad \text{(C-2)}$$

provided that the Fermi level always lies above the surface states level. Referring to Fig. C-1, it can be verified that this condition requires

$$V_{bo} < E_g - V_{ss} - \varphi_n \qquad \text{(C-3)}$$

where V_{bo} is the amount of band-bending in the semiconductor, E_g is the energy gap, and V_{ss} is the surface state energy referred to the valence band. The space charge in the semiconductor, assuming fully-ionized donors in the bulk, is given by

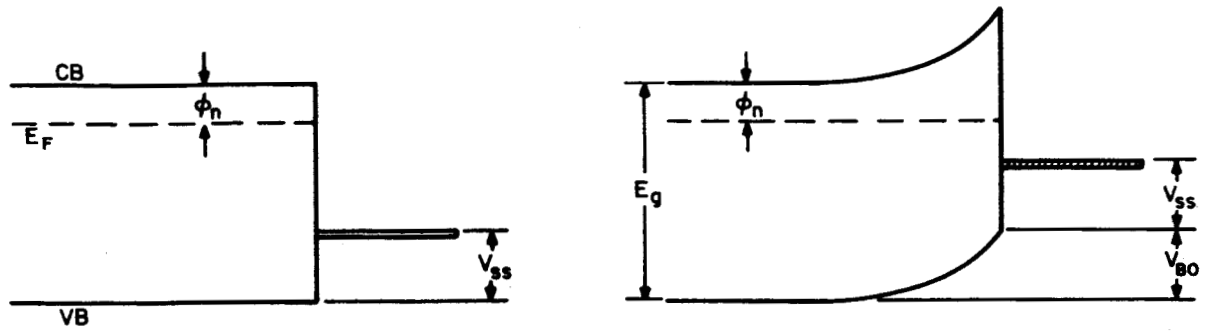

(a) SURFACE STATES EMPTY (b) EQUILIBRIUM: SURFACE STATES FULL

FIG. C-1 ENERGY BAND DIAGRAM FOR A FREE n-TYPE SEMICONDUCTOR SURFACE WITH DISCRETE SURFACE STATES LEVEL. Surface state level has N_{ss} state/cm^2.

$$Q_{sc} = \left[2e\epsilon_s N_d \left(V_{bo} - \frac{kT}{e}\right)\right]^{\frac{1}{2}} \qquad \text{coul/cm}^2 \qquad \text{(C-4)}$$

where ϵ_s = semiconductor dielectric constant, and N_d = donors/cm^3. Substitution of (C-2) and (C-4) into (C-1) results in an equation from which V_{bo} can be found as

$$V_{bo} = \frac{eN_{ss}^2}{2\epsilon_s N_d} + \frac{kT}{e} \quad . \qquad \text{(C-5)}$$

2. Metal-Semiconductor Contact

Figure C-2 shows the band diagram of a metal n-type semiconductor contact. Inspection of the diagram readily shows the following equation to be valid:

$$\varphi_n + V_{bo} + E_A + \Delta_o = \varphi_m \quad . \qquad \text{(C-6)}$$

If Δ_o, the potential drop across the interfacial layer, is regarded as positive when a negative surface charge Q_m appears on the metal, then by Gauss' law

$$\Delta_o = -\frac{\delta}{\epsilon_i} Q_m \qquad \text{(C-7)}$$

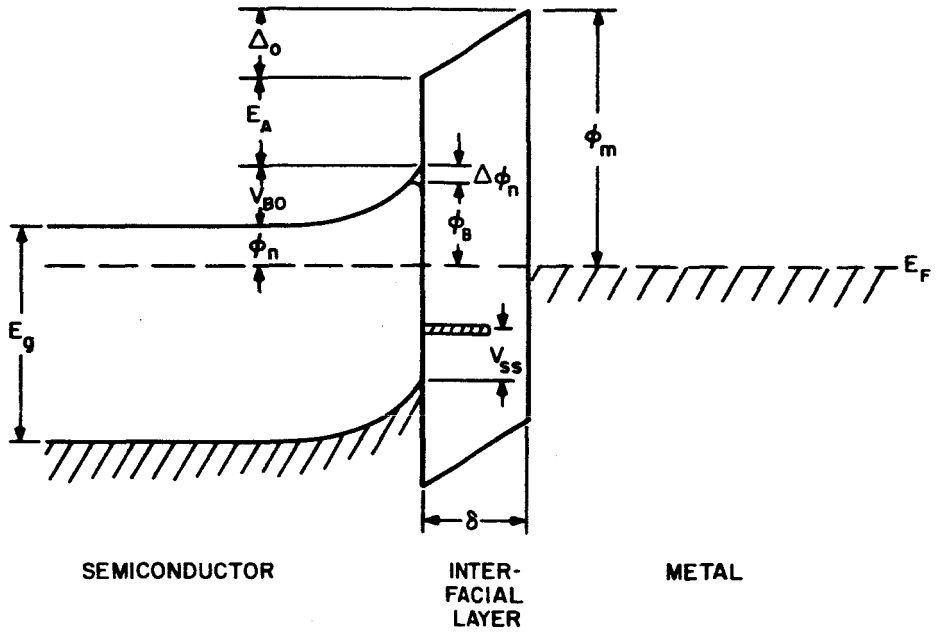

FIG. C-2 ENERGY BAND DIAGRAM FOR A METAL-n-TYPE SEMICONDUCTOR CONTACT WITH DISCRETE SURFACE STATES LEVEL LOCATED V_{ss} ev ABOVE VALENCE BAND

where δ and ϵ_i are the thickness and permittivity of the interfacial layer, respectively. From the requirement for overall charge neutrality, we have

$$Q_m = - (Q_{ss} + Q_{sc}) \qquad \text{(C-8)}$$

so that

$$\Delta_o = \frac{\delta}{\epsilon_i} (Q_{ss} + Q_{sc}) \quad . \qquad \text{(C-9)}$$

Using (C-2) and (C-4) this becomes

$$\Delta_o = \frac{\delta}{\epsilon_i} \left\{ - eN_{ss} + \left[2e\epsilon_s N_d \left(V_{bo} - \frac{kT}{e} \right) \right]^{\frac{1}{2}} \right\} \quad . \qquad \text{(C-10)}$$

Rewriting (C-6) as

$$\Delta_o = (\varphi_m - \varphi_n - E_A) - V_{bo} \qquad \text{(C-11)}$$

we now have two equations, (C-10) and (C-11), which can be combined and solved for V_{bo}. Introducing the definitions

$$V_1 = 2e\epsilon_s N_d \frac{\delta^2}{\epsilon_i^2} \tag{C-12}$$

$$V_2 = \frac{kT}{e} \tag{C-13}$$

$$V_3 = e \frac{\delta}{\epsilon_i} N_{ss} \tag{C-14}$$

we obtain

$$[V_1(V_{bo} - V_2)]^{\frac{1}{2}} = \varphi_m - \varphi_n - E_A + V_3 - V_{bo} \tag{C-15}$$

by equating (C-10) and (C-11). Equation (C-15) can now be solved for V_{bo}. For low enough donor densities, ($N_D \leq 10^{17}$ cm^{-3}), an approximation to (C-15) can be made: The quantity V_1 defined above is found to be on the order of 0.01 ev if $\delta \approx 10\text{Å}$ and $\epsilon_i \approx \epsilon_o$; and since V_{bo} is on the order of one volt, the left hand side of (C-15) is on the order of 0.1 ev. It is therefore not a bad approximation to write

$$V_{bo} \simeq \varphi_m - \varphi_n - E_A + V_3 \tag{C-16}$$

or in terms of φ_b:

$$\varphi_b \simeq \varphi_m - E_A + V_3 - \Delta\varphi_n \tag{C-17}$$

where $\Delta\varphi_n$ is the image force lowering of the barrier. Figure C-3 shows Eq. (C-17) plotted for silicon, taking $E_A = 4.01$ ev[2] and $V_1 \simeq 0.01$ ev. The quantity V_3 is chosen to make Eq. (C-17) agree with the curve in Fig. B-5, and is found for this case to be 0.2 ev. The dashed line in Fig. C-3 represents the exact solution of Eq. (C-15) for the same choice of parameters, showing that little error is incurred in using the more convenient approximate form, Eq. (C-17).

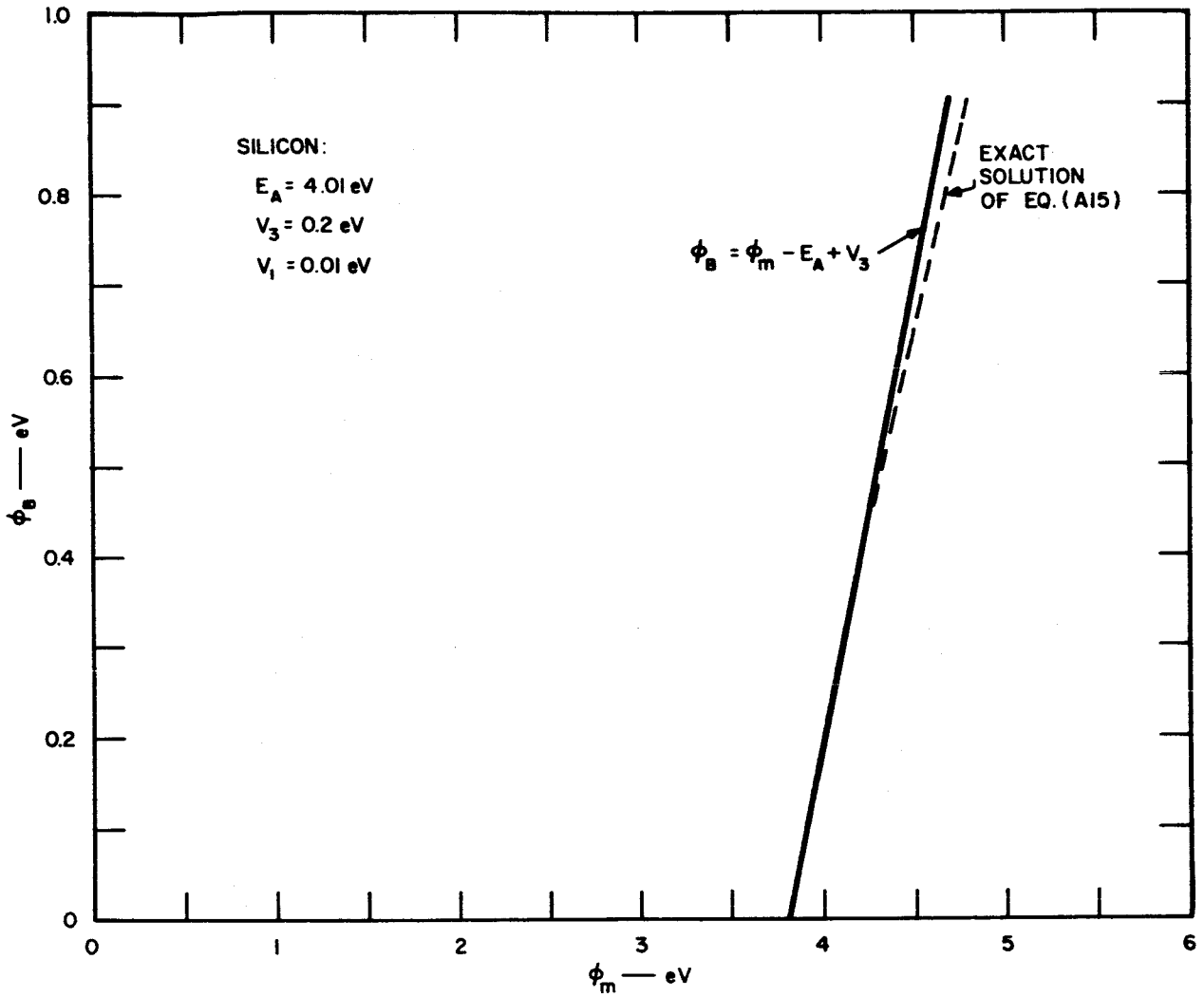

FIG. C-3 BARRIER HEIGHT vs. WORK FUNCTION FOR SILICON-METAL SYSTEM WHERE SURFACE STATE LEVEL REMAINS BELOW FERMI LEVEL

It should be clear at this point that the assumption of a discrete surface-states level is not necessary in the preceding derivations; it is sufficient that all surface states, regardless of their distribution in energy, lie more than kT/e volts below the Fermi level at the surface. This insures that Q_{ss} remains constant as different metals are used to form the contact.

3. Barriers with $V_{bo} \geq E_g - V_{ss} - \varphi_n$

In considering what happens when (C-3) is not fulfilled, i.e., when the Fermi level at the surface enters the energy region of high surface

states density, it is convenient again to assume the discrete surface states level. The behavior of the contact as the metal work function φ_m is increased beyond that value which makes

$$V_{bo} \approx E_g - V_{ss} - \varphi_n \qquad \text{(C-18)}$$

is easily understood: V_{bo} remains "pinned" to the value given in (C-18), and the change in contact potential difference between metal and semiconductor, necessitated by the increase in φ_m, is provided by the emptying of the surface states level which allows all the change in potential to occur across the interfacial layer. Figure (C-4) has been prepared from Eq. (C-17) for GaAs, with $E_A = 4.07$ ev^2, $V_3 = 0.5$ ev, $V_1 \simeq 0.01$ ev. If V_{ss} is taken to be about 0.55 ev, i.e., the surface state level is located 0.55 ev from the valence band, then the curve in Fig. (C-4) bends toward the horizontal for barriers of about 0.85 to 0.90 ev. Comparing Fig. (C-4) and Fig. B-7, it can be seen that this model provides a reasonable explanation for the deviation of the Au and Pt points from the "Schottky" relation line, $\varphi_b = \varphi_m - 3.57$.

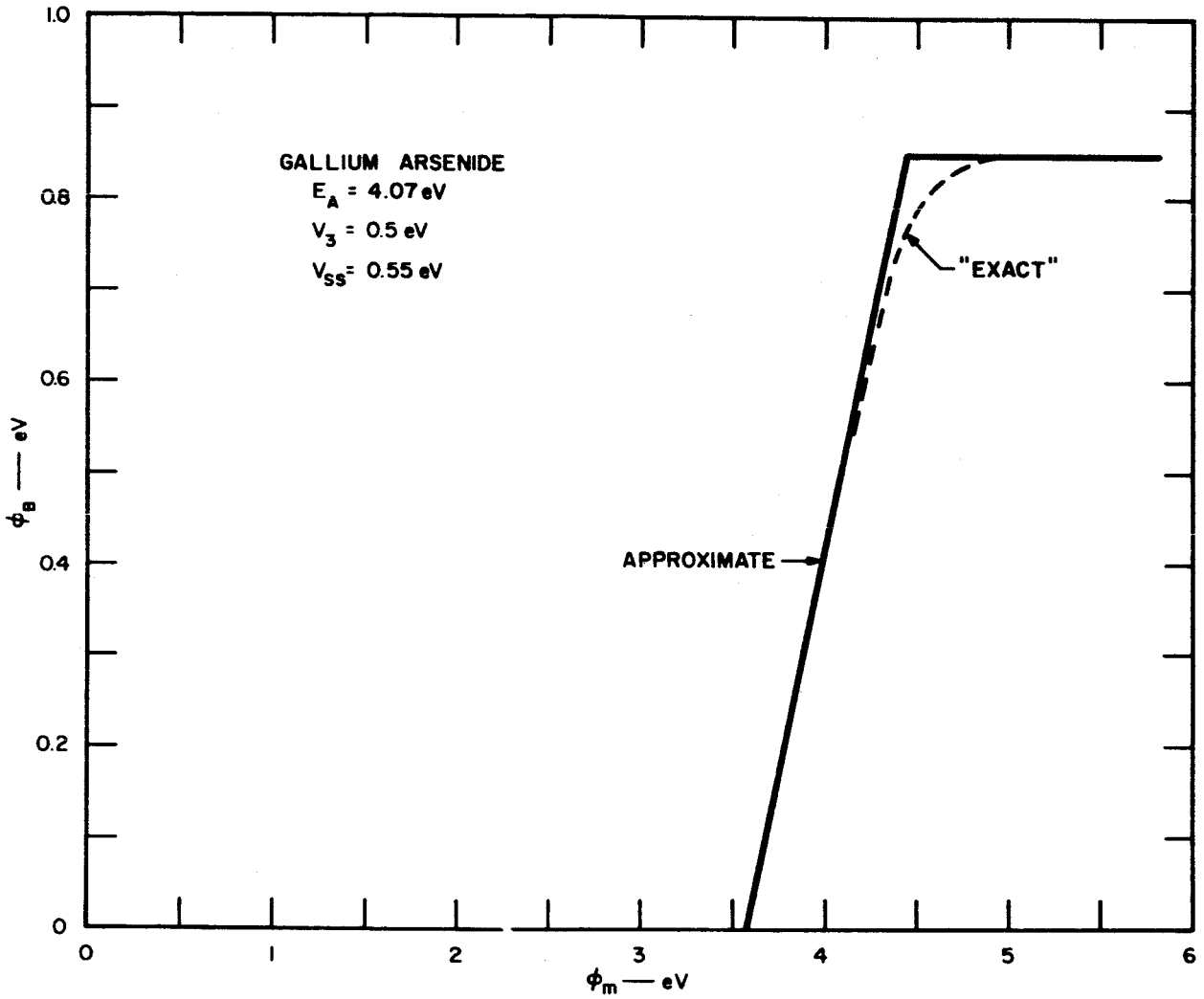

FIG. C-4 BARRIER HEIGHT vs. WORK FUNCTION FOR GaAs-METAL SYSTEM WHERE FERMI LEVEL ENTERS REGION OF HIGH SURFACE STATE DENSITY N_{ss} (E) FOR HIGHER WORK FUNCTION METALS

REFERENCES

1. J. Langmuir and J. B. Taylor, Phys. Rev. 44, p. 423 (1923).

2. C. N. Berglund, W. E. Spicer, Phys. Rev. 136, p. A1044 (1964).

3. J. M. Houston, Bull. Am. Phys. Soc. 6, Ser. II, p. 358 (1961).

4. E. R. Gyftopoulos and J. D. Levine, J. Appl. Phys. 33, p. 67 (1962).

5. G. E. Moore and H. W. Allison, Phys. Rev. 77, p. 246 (1950).

6. T. S. Kirsanova and A. R. Shul'man, Soviet Physics-Solid State 6, p. 225 (1964).

7. L. R. Koller, Phys. Rev. 33, p. 1082 (1929).

8. C. H. Prescott and M. J. Kelly, Bell Syst. Tech. J. 11, p. 334 (1932).

9. N. R. Campbell, Phil. Mag. 12, p. 173 (1931).

10. W. G. Spitzer, C. R. Crowell, M. M. Atalla, Phys. Rev. Letters 8 p. 57 (1962).

11. C. R. Crowell, W. G. Spitzer, L. E. Howarth, and E. E. LaBate, Phys. Rev. 127, p. 2006 (15 September 1962).

12. S. M. Sze, J. L. Moll, and T. Sugano, Solid State Electron. 6, p. 509 (1964).

13. S. M. Sze, Stanford Electronics Laboratory Technical Report No. 1659-4 (April 1963).

14. P. Bardell, Stanford Electronics Laboratory Technical Report No. 5059-1 (August 1964).

15. R. W. Soshea and R. C. Lucas, Phys. Rev. (To be published.)

16. C. A. Mead and W. G. Spitzer, Phys. Rev. Letters 10, p. 471 (1963); Phys. Rev. 134, p. A713 (1964).

17. A. M. Cowley and S. M. Sze (To be published.)

18. N. B. Hannay, Semiconductors, p. 52 (Reinhold, New York, 1959).

19. M. Cowley and H. Heffner, J. Appl. Phys. 35, p. 255 (1964).

20. D. V. Geppert, B. V. Dore, Stanford Research Institute Technical Report AFAL-TR-65-56, Project 4812, "Thin-Film Cold Cathodes for Microwave Tubes," p. 16 (February 1965).

21. A. M. Goodman, J. Appl. Phys. 35, p. 573 (1964); Surface Science 1, p. 54 (1964).

22. W. G. Spitzer and C. A. Mead, J. Appl. Phys. 34, p. 3061 (1963).

23. R. H. Bube, Photoconductivity of Solids, pp. 269-270 (Wiley, New York, 1960).

24. J. H. deBoer, The Dynamical Character of Absorption, Ch. 2 (Oxford, 1953).

25. L. J. van der Pauw, "A Method of Measuring Specific Resistivity and Hall Effect of Discs of Arbitrary Shape," Philips Research Reports, 13, No. 1, pp. 1-9 (February 1958).

26. T. M. Dauphinee and E. Mooser, "Apparatus for Measuring Resistivity and Hall Coefficient in Semiconductors," Rev. of Sci. Inst. 26, No. 7 (1955).

27. A. L. Hughes and L. A. Dubridge, Photoelectric Phenomena, p. 241 (McGraw-Hill, 1932).

28. R. H. Fowler, Phys. Rev. 38, p. 45 (1931).

29. R. H. Fowler, Statistical Mechanics, p. 342 (Cambridge, 1955).

30. L. A. DuBridge, Phys. Rev. 43, p. 727 (1933).

31. H. B. Michaelson, J. Appl. Phys. 21, p. 536 (June 1950).

32. G. W. Gobeli and F. G. Allen, Phys. Rev. 137, p. A245 (1965).

33. N. B. Kindig, Tech. Report No. 5201-1, Solid State Electronics Laboratory, Stanford University, Stanford, California (August 1964).

34. R. J. Archer and M. M. Atalla, Annals N.Y. Acad. Sci. 101, p. 697 (1963).

35. R. Suhrmann and G. Wedler, Zeitz. für Angew. Physik 14, p. 270 (1962).

36. S. M. Bryla and C. Feldman, J. Appl. Phys. 33, p. 774 (March 1962).

37. H. E. Farnsworth, Proc. Phys. Soc. 71, p. 703 (April 1958).

38. Chung Fu Ying and H. E. Farnsworth, Phys. Rev. 85, p. 485 (1952).

39. R. Culver, J. Pritchard, and F. C. Tompkins, Zeits. für Elektrochemie 63, p. 741 (1959).

40. J. C. Revière, Proc. Phys. Soc. London B70, p. 676 (1957).

41. P. A. Anderson, Phys. Rev. 115, p. 553 (1 August 1959).

42. J. S. Anderson and D. F. Klemperer, Royal Soc. Proc. 258, p. 350 25 October 1960).

43. H. B. Michaelson, "Electron Work Functions of the Elements," Handbook of Chemistry and Physics, 45th Edition (1964-65).

44. J. R. Stevenson and E. B. Hensley, J. Appl. Phys. 32, p. 166 (February 1961).

45. R. A. Chapman, J. Appl. Phys. 35, p. 2832 (October 1964).

46. For an account of this work, see F. G. Allen and G. W. Gobeli, Phys. Rev. 127, p. 150 (1962), and references contained therein.

47. E. O. Kane, Phys. Rev. 127, p. 131 (1962).

48. J. Van Laar and J. J. Scheer, Proc. Int. Conf. on Physics of Semiconductors (Exeter, July 1962).

49. J. J. Lander, G. W. Gobeli, J. Morrison, J. Appl. Phys. 34, p. 2298 (1963).

50. J. J. Scheer and J. Van Laar, Phys. Letters 3, p. 246 (1963).

51. W. Shockley, Phys. Rev. 56, p. 317 (1939) and references contained therein.

52. See, for example, Refs. 32 and 46.

53. J. Bardeen, Phys. Rev. 71, p. 717 (1947).

54. V. Heine, Phys. Rev. 138, p. A1689 (1965).

55. F. G. Allen and G. W. Gobeli, J. Appl. Phys. 35, p. 597 (1965).

56. D. Kahng, Bell Syst. Tech. J. 43, p. 215 (1964).

STANFORD
RESEARCH
INSTITUTE

MENLO PARK
CALIFORNIA

Regional Offices and Laboratories

Southern California Laboratories
820 Mission Street
South Pasadena, California

Washington Office
808–17th Street, N.W.
Washington 6, D.C.

New York Office
270 Park Avenue, Room 1770
New York 17, New York

Detroit Office
1025 East Maple Road
Birmingham, Michigan

European Office
Pelikanstrasse 37
Zurich 1, Switzerland

Japan Office
c/o Nomura Securities Co., Ltd.
1–1 Nihonbashidori, Chuo-ku
Tokyo, Japan

Representatives

Toronto, Ontario, Canada
Cyril A. Ing
Room 710, 67 Yonge St.
Toronto 1, Ontario, Canada

Milan, Italy
Lorenzo Franceschini
Via Macedonio Melloni, 49
Milano, Italy